

Review

Recent Applications of Ionic Liquids in the Sol-Gel Process for Polymer–Silica Nanocomposites with Ionic Interfaces

Katarzyna Z. Donato ^{1,2}, Libor Matějka ³, Raquel S. Mauler ² and Ricardo K. Donato ^{1,*} 

¹ MackGraphe (Graphene and Nano-Material Research Center), Mackenzie Presbyterian University, Rua da Consolação 896, São Paulo 01302-907, SP, Brazil; zawada.kat@gmail.com

² Institute of Chemistry, Universidade Federal do Rio Grande do Sul (UFRGS), Av. Bento Gonçalves 9500, P.O. Box 15003, Porto Alegre 91501-970, RS, Brazil; raquel.mauler@ufrgs.br

³ Institute of Macromolecular Chemistry, Heyrovský Sq. 2, 162 06 Prague, Czech Republic; matejka@imc.cas.cz

* Correspondence: ricardo.donato@mackenzie.br; Tel.: +55-11-2766-7385

Received: 21 October 2017; Accepted: 5 November 2017; Published: 10 November 2017

Abstract: Understanding the organic–inorganic interphases of hybrid materials allows structure and properties control for obtaining new advanced materials. Lately, the use of ionic liquids (ILs) and poly(ionic liquids) (PILs) allowed structure control from the first sol-gel reaction steps due to their anisotropy and multiple bonding capacity. They also act as multifunctional compatibilizing agents that affect the interfacial interactions in a molecular structure-dependent manner. Thus, this review will explore the concepts and latest efforts to control silica morphology using processes such as the sol-gel, both in situ and ex situ of polymer matrices, pre-polymers or polymer precursors. It discusses how to control the polymer–filler interphase bonding, highlighting the last achievements in the interphase ionicity control and, consequently, how these affect the final nanocomposites providing materials with barrier, shape–memory and self-healing properties.

Keywords: ionic liquids; sol-gel; ionic interfaces; polymer nanocomposites; hybrid materials; barrier properties; shape–memory; self-healing

1. Introduction

Hybrid materials produced via sol-gel process allow the permanent incorporation of organic groups in inorganic systems, integrating both properties of the components. Sol-gel process also permits preparation of new materials with high purity and homogeneity under relatively mild conditions. A better understanding of the organic–inorganic interfaces of sol-gel based hybrid materials allows structure and properties control, thus been extremely important when new advanced materials syntheses are in focus. The interface tuning allows creating hybrid materials with properties that are not only the sum of individual contributions of both phases, but specific and unique for the system [1].

Many studies have reported that, besides the pH, temperature and concentration effects, applying ionic and/or highly anisotropic compounds into the sol-gel system can cause significant changes [2]. Among those, the use of ionic liquids (ILs), due to their ionicity, anisotropy and multiple bond capacity, have shown to allow structure control. Perhaps most importantly, the ILs present the most dramatic effects when applied in the first sol-gel process steps, both in simple or complex gel growth [3–5]. Thus, the understanding of the sol-gel hydrolysis and condensation steps, and the basic parameters controlling them, is necessary for unveiling the IL's role.

It has been shown that both, the ex situ application of pre-formed sol-gel silica-IL hybrids in melted thermoplastics [6] and in situ formation in thermosets [4,7–10] or water soluble polymers [11] improve significantly thermo–mechanical properties of polymer matrices. In those systems ILs act

as multifunctional compatibilizing agents that affect the interfacial interactions, which becomes dependent on the IL's molecular structure, morphology and functional groups. Therefore, controlling the applied IL molecular structure allows also tuning the nanocomposites' final properties.

2. Hybrid Silica Materials via Sol-Gel Process

Sol-gel describes hydrolysis and condensation processes and covers the synthesis of solid materials, such as metal oxides, from solution-state precursors. Its main advantage is the feasible synthesis tuning by changing and monitoring reaction parameters (e.g., pH, catalyst, temperature and/or reactants concentration) [2], and forming species with controllable nanoscale architecture, unique morphologies and properties. Thus, it is a constant source of new surface and interphase controlled materials that allows physicochemical properties adjustment under mild reaction conditions [12]. Moreover, potential functionalities can be easily expanded by organic functional groups incorporation into the inorganic matrix. Hybrid inorganic–organic materials formed in such a way are more adaptable to materials engineering, producing specific properties for the vast application range; e.g., hybrid coatings [13], biohybrids [14] and materials for medical applications [15].

The strategies for the synthesis of hybrid sol-gel materials are extensively discussed in the literature [1,16,17], however, two main synthesis pathways are presented; (i) one-pot synthesis (co-condensation) and (ii) post-synthesis (silylation). The main difference between those two strategies is the organic modification degree. In the co-condensation method, the organic groups are grafted into the inner and outer pore walls during their formation and the organic limit for this modification is 40 mol % for avoiding pore disorganization. When functionalization occurs after the pore formation, the organic modifier is attached only to the outer pore walls, thus the organic limit can be higher [15]. In these systems, the interphase properties play an important role in establishing the final material's function. Based on the interphase type, the sol-gel process allows the formation of two main classes of hybrid materials. In the first one, inorganic and organic components are incorporated with weak (noncovalent) bonds, including ionic interactions, hydrogen bonding (H-bonding), van der Waals forces and π - π interactions [1]. An example of the first class is the organic molecule "imprisonment" into the formed inorganic network cavities, in an extremely homogenous manner. The pigment rodamine 6G [18], pyrene [19] or enzymes [20] are only a few examples of organic molecules that could be successfully imprisoned into the silica matrix. However, in the second class, two phases are strongly (covalent and/or ionocovalent) bonded. The preparation of organically modified alcoxysilane precursors, i.e., $R'nSi(OR)_{4-n}$ or $(OR)_4-nSi-R''-Si(OR)_{4-n}$ ($n = 1, 2, 3$), and their use in hydrolysis and condensation steps, is an example of this class. In this case, organofunctionalized group (-R') affects the inorganic network formation depending on its chemical structure [21].

3. Ionic Liquids

Ionic liquids (ILs) are organic salts with melting temperature (T_m) ≤ 100 °C, which present ionocovalent structures and belong to the multifunctional agents' class. The IL molecules are constituted of counter ions and are often liquid at room temperature [22,23]. In comparison to the traditional salts e.g., NaCl, the ILs usually contain bulky organic cations with low symmetry degree (Figure 1). The cation's asymmetry and charge dislocation result in weak electrostatic interactions, decreasing the T_m [22]. The ions' size can drastically influence the T_m . For example, the NaCl contains small ions that allow the formation of a compact crystalline resulting in a high T_m , while larger ions, such as bis(trifluoromethylsulfonyl)imide [NTf₂] or hexafluorophosphate [PF₆], make crystalline packing less efficient, thus significantly decreasing the T_m . Also the increase in the cation alkyl side chain length causes an increase in T_m (Table 1) [24].

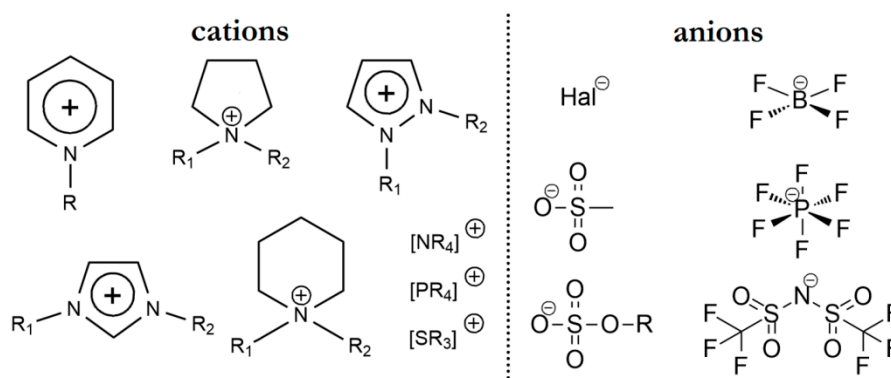


Figure 1. Commonly used ILs cations and anions, where $[NR_4]$, $[PR_4]$ and $[SR_3]$ represent different structures of ammonium, phosphonium and sulphonium respectively, and Hal^- represent the halogens group.

Table 1. Melting temperature (T_m) of common inorganic salts in comparison to ILs based on 1-alkyl-3-methylimidazolium $[C_nMIm]$ cations and chloride $[Cl]$, hexafluorophosphate $[PF_6]$ or bis(trifluoromethylsulfonyl)imide $[NTf_2]$ anions.

		T_m ($^{\circ}C$)
Inorganic Salts	NaCl	803
	KCl	772
Ionic Liquids	$[C_4MIm][Cl]$	68 *
	$[C_4MIm][NTf_2]$	-4 *
	$[C_4MIm][PF_6]$	10 *
	$[C_{10}MIm][PF_6]$	32 *
	$[C_{16}MIm][PF_6]$	75 *

* Values obtained from reference [24].

There are two main IL classes that differ by the synthesis type, which involve the proton transference (protic ILs) or an alquilation process (aprotic ILs). Gabriel and Weiner reported in 1888 what was probably the first protic IL, Ethanolammonium nitrate (m.p. 52–55 $^{\circ}C$) [25]. Only almost 30 years later, in 1914, Walden synthesized the first protic room temperature IL via neutralization of ethylamin with HNO_3 , forming ethylammonium nitrate ($T_m = 12$ $^{\circ}C$) [26]. In 1951, Hurley and Wier produced an aprotic IL using ethylpyridinium bromate and aluminum chloride. The cations were derived from organic components via alquilation with alkyl halide [27]. However, these ILs are not used nowadays since they are sensitive to moisture. The first water-stable ILs were synthesized by Wilkes and Zaworotko in 1992 and contained tetrafluoroborate $[BF_4]$, hexafluorophosphate $[PF_6]$, nitrate $[NO_3]$, sulphate $[SO_4]$ or acetate $[C_2H_3O_2]$ anions; although the hydrolysis of $[BF_4]$ and $[PF_6]$, forming fluoridric acid (HF), was later reported disproving this claim. From that moment on, a large number of ILs with organic cations and inorganic or organic anions were obtained and studied [22,24]. The most typical cations comprised of aromatic nitrogen containing heterocycles, e.g., imidazole, pyrrole and pyridinium, or acyclic cations e.g., ammonium, phosphonium and sulphonium (Figure 1).

Depending on their structures, ILs may present many desirable properties such as low volatility, corrosivity and flammability, high thermal and chemical stability, good thermal conductivity and ionic mobility [22]. These properties have being exploited in many applications like solvents for organic reactions and bioscience (i.e., cellulose dissolution) [28], combustion and solar cells and as catalysts or electrolytes for batteries [23]. Moreover, the ILs' application fields are constantly expanding due to their large number of possible structural modifications. Specific structural changes, like cation functionalization (with alkyl chains of different length or polar groups) or anion exchange, can cause variations in many properties, such as viscosity, ionic conductivity and solubility, as well as

in the degradation (T_d) and glass transition (T_g) temperatures [22,29,30]. For example, side chain length increase from $-C_4H_9$ to $-C_{10}H_{21}$ of 1-alkyl-3-methylimidazole cation caused T_d reduction [24]. Another example would be the expressive increase in water solubility and decrease in the T_d after exchanging the hydrophobic $[NTf_2]$ anion by the more hydrophilic $[BF_4]$ [24]. The IL's functionalization with polar groups (e.g., ether-, carboxy- or alcohol-) has been attracting considerable attention for areas like deep-eutectic solvents, electrochemistry and materials with biological interfaces [30,31]. The introduction of polar groups leads to reduced viscosity, crystallinity, T_m and T_g , as well as increased polarity, hydrophilicity and hydrogen-bonding capability among IL molecules [32], when compared to their aliphatic analogs [33,34]. Moreover, another structure variation can be caused by competitions between the cation–cation (e.g., ether–ether) and cation–anion interactions, resulting in cation dimers formation [35,36]. The ILs are also used in areas like bioscience and bioengineering since they present antimicrobial [37–39], antitumoral, antioxidant [40] properties and have low toxicity to human leucocytes [38], especially when derived from the imidazolium cation. Imidazolium salts can also be found in nature, e.g., Lepidiline A and B that are present in the Peruvian maca roots, *Lepidium meyenii*, and demonstrate anticancer properties [41].

Due to their biodegradability [42], ILs are frequently referred to as green solvents [43], as they help reducing the use of volatile, dangerous and pollutant organic solvents, making especially the new materials synthesis more environmentally friendly. Moreover, based on their unique physicochemical properties, the ILs application in the new materials synthesis produce distinct morphologies and properties not accessible with the use of common organic solvents or water. A significant increase in radical polymerization reaction efficiency was observed when IL was used as reaction medium instead of other polar/coordinative solvents. In the case of atom transfer radical polymerization (ATRP) and reversible addition/fragmentation chain-transfer polymerization (RAFT), ILs facilitated the separation between polymer and residual catalyst as well as reduced the number of side reactions [44–48]. Their capacity to preserve high ionic conductivity up to the decomposition temperature propelled many studies where electrolyte matrices were developed. In order to perform this, ILs were physically or chemically gelled with the low molecular weight components, inorganic particles or carbon nanotubes to form quasi-solid ion conductive electrolytes [49–53].

Also, the ILs solidification by polymers and production of highly conductive polymeric gel have been recently developed. These conductive polymeric gels can be divided in three types: (i) polymers doped with ILs, where, only part of the system is solubilized by the IL; e.g., an ABA triblock copolymer can be doped with IL which is capable to solubilize B block at low temperatures while immiscible A blocks aggregate due to phase separation and form a ionogel. The system will present thermoreversible gelation if block A is soluble in IL at high temperatures [54,55]. (ii) in situ polymerization of vinyl monomers in ILs, where the molecularly dispersed monomers polymerize to form a homogeneous network swelled by IL medium, forming ionogels [56]. (iii) ILs polymerization, where polymerizable groups are covalently introduced into the IL's cation or anion structures. In this way, the IL itself will become the cross-linked ionogel. A great variety of polymerizable ILs was reported in the literature, some of them include polycation, polyanion, copolymer and poly(zwitterion) ILs [55,57].

Moreover, many ILs can be used in polymer systems as plasticizers, lubricants, strengthening or interfacial agents, causing improvements in barrier, mechanical and thermal properties [58,59]. Furthermore, the effect as morphology drivers/templates in ceramic nanoparticles formation [5,60–67] and their further use in compatibilizing various polymer nanocomposites [4,6–9,11] have been extensively investigated.

4. Molecular Imprinting in the Sol-Gel Process Using Ionic Liquids

Besides all the control options available by changing the sol-gel process parameters, it is also possible to obtain differentiated structures when organic components are used as templates. The gel formation over a template that can be further removed allows molding the final material's morphology. This process is referred in various studies as molecular imprinting, nanocasting or

lost-wax method [68–71]. Two 3D molecular imprinting methods, which are dependent on the organic–inorganic interphase, are often used: (i) for noncovalent-bonded interphases, the imprinting regions can be produced by the template–matrix affinity. Applied sol-gel precursor should then form an enough porous matrix for allowing the template’s extraction after the drying process (Figure 2a); (ii) for interphases with reversible covalent bonds, the polymerization of organically modified alcoxysilane precursor (precursor–template or precursor–sacrificial spacer) can be used in excess. Then, the template or sacrificial spacer can be chemically removed, leaving free specific sized spaces (Figure 2b) [70].

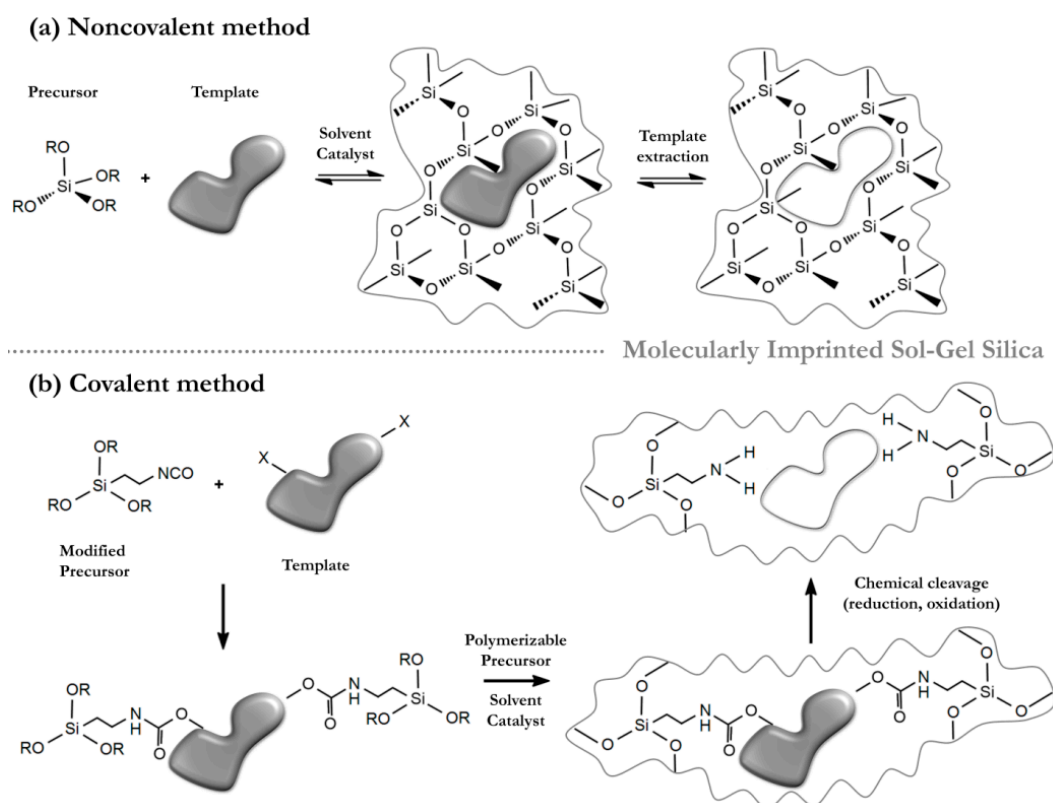


Figure 2. Molecular imprinting methods in sol-gel process (a) noncovalent templating and (b) covalent templating [70] (permission obtained for reproduction).

The application of templates in molecular imprinting offers broad range of 3D matrices in different configurations. Thin films, porous materials or bulk structures are just examples that can be used as adsorbents or separation materials, catalysts or sensors. Many modeling (templating) techniques are discussed in the literature, using a broad variety of solvents, surfactants [71,72], even natural products (Figure 3) [73]. Moreover, the effect of these molecules into the sol-gel development is so intrinsic that the final gel will inherit the natural ordering of entrapped molecules. A very illustrative example can be given by the entrapment of chiral molecules. Depending on how a chiral template is applied to the sol-gel process it can lead to the formation of quiral pores [74] that after the template removal will be selective for that enantiomer used [75], or even the whole gel structure can self-assemble to a helical structure obeying the template’s chirality (Figure 3c) [76].

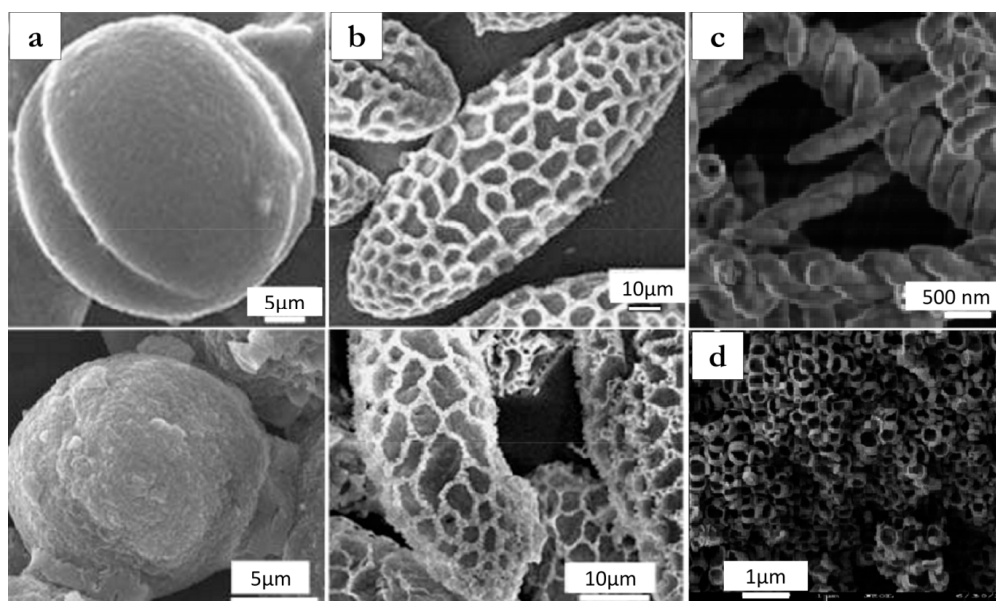


Figure 3. Molecular imprinted materials and their surface structure diversity. SEM images of (a) camellia and (b) rapeseed pollens (top) with their molecular impressions (bottom) [73] (permission obtained for reproduction); (c) chiral helical structure formed by a chiral low molecular weight gelators as templates [76] (Reprinted from Ref. [76] with permission of The Royal Society of Chemistry.) and (d) macroporous silica used for biodiesel synthesis where liquid crystalline surfactants and polystyrene beads were used as templates [72] (Reprinted from Ref. [72] with permission of The Royal Society of Chemistry.).

In the sol-gel process, ILs not only act as templates, but have ability to stabilize the structures formed, working as efficient templates/solvents [67] and, in some cases templates/solvents/reactants [77]. The first attempt to substitute common organic solvents with ILs, as a reaction medium/template for inorganic materials' formation via sol-gel method, was successfully performed by Dai et al. in 2000 [78]. They applied 1-*n*-ethyl-3-methylimidazolium bis(trifluoromethylsulfonyl)imide [$C_2MIm][NTf_2]$] for the gel formation using tetramethyl orthosilicate (TMOS) as the silica precursor and a formic acid excess as the catalyst. The gel formed by this method is often called as ionogel and it results in two interpenetrating continuous 3D networks, i.e., an IL phase confined into the gel's scaffold [66]. The IL was then extracted, leaving porous structure with high specific surface area (similar to those in aerogels $720 \text{ m}^2/\text{g}$) without the need of using supercritical solvents. Additionally, modifying the IL/silica ratio allowed controlling the pore size, providing a versatile method for high porosity gels preparation [78]. From that moment on, a countless number of new hybrid materials synthesized via sol-gel method using ILs as solvents [21,79], co-solvents [80,81], surfactants, drying controllers [81], crystals growth modifiers [82], as well as templates [61–65,67] emerged. Kinoshita et al. observed, using the sol-gel method with 1-*n*-ethyl-3-methylimidazolium tetrafluoroborate [$C_2MIm][BF_4]$] or 1-*n*-butyl-3-methylimidazolium tetrafluoroborate [$C_4MIm][BF_4]$] as solvents, a higher $Al(OH)_3$ crystallinity when a longer alkyl side chain was applied [82]. Seddon et al. reported the formation of mesoporous silica (MCM-41) with hexagonal structure, prepared in lightly basic conditions, by substituting the traditional template, alkyltrimethylammonium, with ILs based on 1-alkyl-3-methylimidazolium [C_nMIm] cation. It allowed obtaining the porosity and crystallinity characteristic for MCM-41 adding an improved lamellar ordering, showing the viability of ILs use in this type of synthesis [65]. Klingshirn et al. used [$C_4MIm][Cl]$] as a chemical additive to control the drying process, thus the sol-gel silica porosity [81]. They observed that this IL formed a non-volatile liquid layer on the pore walls' surfaces. This strengthened the gel walls during the maturation and extraction process (both when using solvent and calcination),

decreasing the risk of structure collapse and forming highly porous morphology. Karout and Pierre showed that adding $[C_4Mim][BF_4]$ during the condensation stage increased the gelification time. Also by changing the IL's concentration the xerogels' and aerogels' pore sizes were controllable [80]. Zhou et al. used 1-hexadecyl-3-methylimidazolium chloride $[C_{16}Mim][Cl]$ as a template for obtaining super-microporous monolithic silica with lamellar ordering [62]. The same group produced highly ordered lamellar and mesoporous titania using 1-*n*-butyl-3-methylimidazolium tetrafluoroborate $[C_4Mim][BF_4]$ and 1-alkyl-3-methylimidazolium chloride $[C_nMim][Cl]$ as templates, which were further removed with acetonitrile or by calcinating at high temperature [64,83]. They also synthesized worm-like mesoporous silica using $[C_4Mim][BF_4]$, and in the same work presented one of the first attempts to explain the silica-IL interaction mechanism. They suggested that an H-bond “co- π - π stacking” mechanism, in which the IL, within the reaction medium, simultaneously self-organizes and interacts with the growing silica domains. This mechanism predicts the simultaneous existence of H-bonds between $[BF_4]$ anions and silica matrix together with imidazolium rings π - π stacking, which resulted in mesoporous silica formation (Figure 4) [61]. Based on that, the geometry, size, polarity and Coulomb coupling forces between anions and cations contribute directly to the final particle size, compactness and morphology (Figure 4) [4,5,60–63,65,79,84,85].

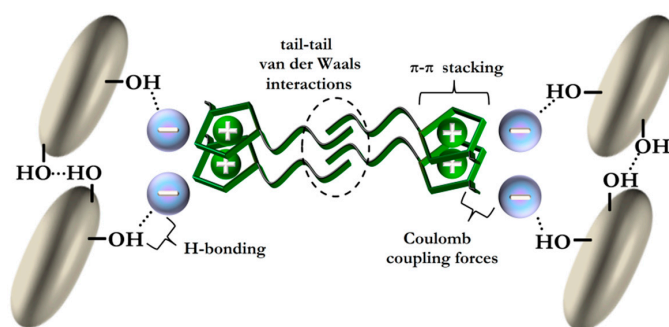


Figure 4. Schematic representation of H-bond “co- π - π stacking” mechanism and the possible interactions among silica and ILs [61] (permission obtained for reproduction).

These studies described mostly the participation of ILs in the sol-gel process only after hydrolysis process and when the condensed phase was dominant in the growing network. However, it is known that the structural behavior of the original solution also determines the polycondensation and network formation in the sol-gel process [2]. Further, a series of studies were performed applying and investigating the influence of different ILs from the first moments of the reaction, allowing further particle structure control [3–5,8,60]. It was observed initially that the use of ILs with 1-ethylene glycol monomethyl ether-3-methylimidazolium $[C_3OMim]$ cation associated to different anions ($[BF_4]$, methanesulfonate $[MeSO_3]$, and hexafluorophosphate $[PF_6]$) resulted in highly distinct morphologies, depending on anion applied. Moreover, further extracting the ILs exposed the ordered porous silica structures formed (Figure 5) [60].

The phase structure evolution in the early stages of the sol-gel process in the presence of ether-functionalized ILs and using two different co-solvents (EtOH and iPrOH) was further investigated by time-resolved FTIR and DLS analyses [3]. A turbid transition period was observed, which was correlated to the water consumption rate and phase structure evolution, and dependent on the IL's cation side chain length, where shorter one produced longer transition periods and larger particles [3,4]. Moreover, in the presence of water, these ILs produced acidic species that promoted the TEOS hydrolysis step [3]. The decrease in reaction times was also observed in later study, where the presence of $[BF_4]$ anion reduced the gelation time (up to 500 \times). In the same work, six different ILs were used as dynamic templates for sol-gel silica synthesis to reduce random agglomeration process. The direct interaction of ILs with growing silica systems was confirmed by microporosity, fractal structuring and morphology changes [5]. To our knowledge, in all systems where ILs were applied

from the beginning of the hydrolytic sol-gel reaction [3–5,60] they accelerated gelation process while presented an opposite behavior when applied after pre-hydrolysis step [80]. It shows an important role of ILs in catalyzing and organizing the sol-gel hydrolysis step, influencing the entire evolution process even when used in very small content.

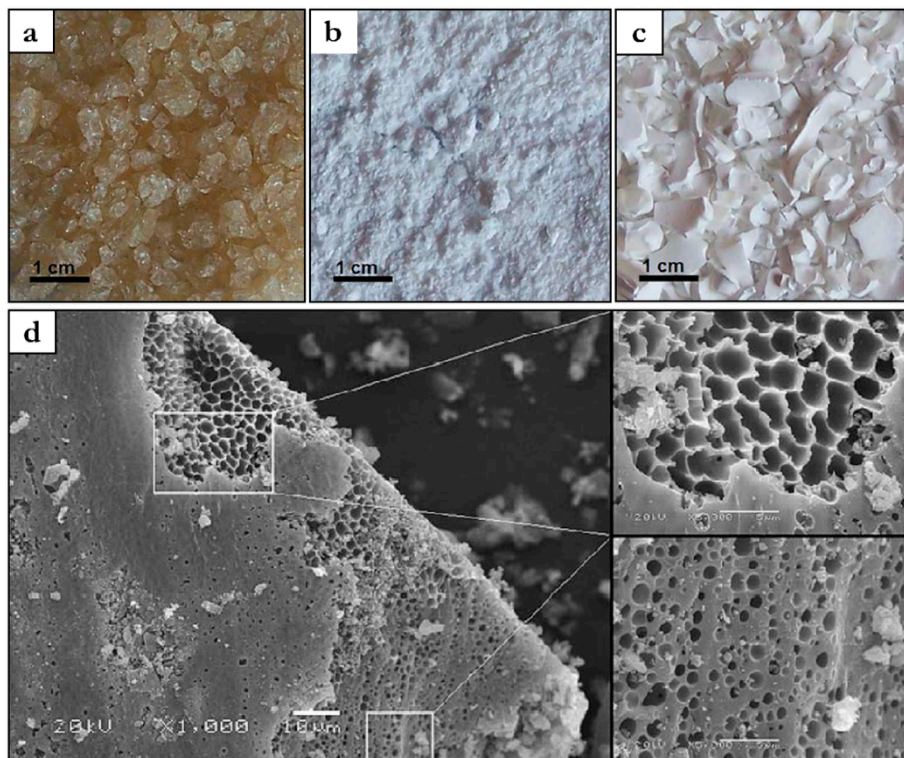


Figure 5. Photographs of silica xerogels synthesized with (a) $[C_3O_1MIm][MeSO_3]$; (b) $[C_3O_1MIm][BF_4]$ and (c) $[C_3O_1MIm][PF_6]$; before grinding and (d) SEM images of silica after $[C_3O_1MIm][PF_6]$ extraction [60] (permission obtained for reproduction).

The use of ILs in non-hydrolytic sol-gel process was also investigated in various studies. Viau et al. prepared non-exuding, crack-free, and transparent monoliths using formic acid solvolysis with $[NTf_2]$ containing ILs. After the extraction obtained porous materials with 10–15 nm and $3\text{ cm}^3/\text{g}$ pore size and pore volumes, respectively [86]. The mixture of TMOS and 1-ethyl-3-methylimidazolium thiocyanate $[C_2MIm][SCN]$ was used by Chandra et al. in non-hydrolytic sol-gel process with high IL loading (85–92 wt %) to prepare tubular spring-like gel structure and porous silica nano-nails after IL extraction [87]. They also studied the use of $[C_2MIm][BF_4]$ and TEOS in different gelation temperatures ($-10, 0, 30\text{ }^\circ\text{C}$). Gels densities, their pore parameters (diameter, surface area, volume and porosity), phase transition temperatures ($T_m, T_c,$ and T_g), IL's thermal stability and vibrational spectra were affected by changes in gelation temperature. Gels prepared at lower temperatures presented higher porosity [88]. Also application of IL into non-hydrolytic sol-gel process accelerates the consumption of TMOS, formic acid and methanol, catalyzing the solvolysis process [89,90].

These materials constitute a new family of thermally-resistant structurally-ordered solids that can be exploited in areas like electrochemistry [21,91,92], catalysis [93,94], biocatalysis, optics, sensors [85], electrorheological fluids [95–97] and nanocomposites preparation [4,6–9,11].

5. Polymer-Sol-Gel Silica Hybrid Nanocomposites

Polymer hybrids are multicomponent heterogeneous systems showing excellent properties in comparison with homogeneous polymer materials or composite polymers containing micro- or

macro-heterogeneities (fillers) in the polymer matrix. In contrast to classical composite materials, the heterogeneity in the polymer nanocomposites or hybrids occurs only on the nano or molecular scale level. The exceptional properties of these systems originate from immense polymer–nanofiller interfacial area and depend on interphase interaction strength. Moreover, the polymer hybrids exhibit optical clarity due to the small size of heterogeneity domains [98].

The organic–inorganic (O–I) polymers involving inorganic components blended in a polymer matrix are typical hybrid materials. Usually, Si, Ti, Sn or Al-based inorganic compounds, are used as inorganic nanofillers. Under optimum conditions, the O–I polymers show both phase properties synergy, i.e., hardness, strength, thermal resistance or non-flammability of the inorganic phase associated to elasticity, toughness and good processability of the polymer. A convenient procedure for organic and inorganic components integration is the conventional sol-gel process technique. It permits preparation of the nanocomposites using both the traditional “top-down” approach, i.e., fillers and polymer matrices synthesized previously, or a self-assembly “bottom-up” processes, e.g., (i) polymerization of alkoxy silanes in a polymer matrix [99,100], (ii) simultaneous in situ formation of filler and polymer matrix [101,102] and also (iii) polymerization of functionalized (alkoxy silane) end-linked polymers [103,104]. The preparation method affects final product properties and the carefully choice of synthesis pathway is crucial when specific properties are desired. Also, effective filler dispersion is a very important aspect since it determines the final nanocomposites’ performance and properties reproducibility. Moreover, for systems presenting weak polymer–filler interaction, the filler–filler interaction prevails and larger inorganic domains are formed, thus disturbing the homogeneity on the small-scale level. Finally, inorganic phase percolation may also occur, leading to a co-continuous O–I phase structure. The silica’s strong interparticle forces cause its agglomeration even when applied as filler into polar matrices, e.g., epoxy resins [105]. In the case of nanocomposites based on low polarity matrices, e.g., polyolefins, the homogeneous polar filler dispersion is an even bigger challenge due to the lower filler-matrix affinity [6,106]. The commonly used techniques for nanosilica dispersion in the polymer matrix can be distinguished as physical and chemical. The physical methods include mixture in solution and processing in molten state, while chemical methods mainly consist on the above mentioned in situ polymerizations variations [107–109]. The disadvantage of solution mixing, where the pre-made particles are dispersed in the polymer solution, is the filler sedimentation and/or agglomeration tendency. Mechanical filler dispersion in molten polymer matrix permits components interaction without the use of a solvent [110]. However, this technique also causes filler agglomeration, especially when polar filler is applied. The manipulation of organic–inorganic interfacial interactions available in the in situ synthesis methods provides more possibilities to overcome the agglomeration problem. Silica preparation via sol-gel process in the presence of a polymer (e.g., in solution or in molten state via reactive extrusion) or *mer* to be polymerized allows obtaining nanocomposites in one or two steps. Mainly alkoxy silanes are used as precursors to generate inorganic structures and tetraethyl orthosilicate (TEOS) is one of the most widely used precursors for in situ silica network formation within an organic matrix (Figure 6).

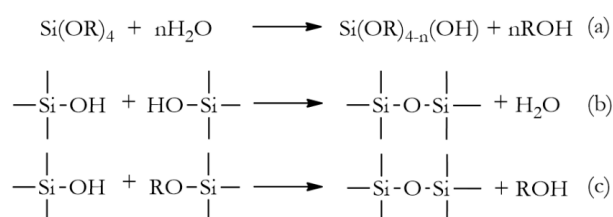


Figure 6. Schematic representation of an alkoxy silane’s hydrolysis (a); hydrolytic condensation (b) and alcohol condensation (c) steps.

The sol-gel process is sensitive to reaction conditions, such as catalysts, water concentration, solvent, etc. While acid catalysts promote mainly hydrolysis, the basic catalysis promotes more

polycondensation [2]. In this process, the selection of the silica domains growth mechanism (i.e., monomer–cluster or cluster–cluster) is an important factor for good filler dispersion. It was found that the tendency of forming smaller silica domains in cluster–cluster mechanism makes it more favorable for the homogeneous nanocomposite formation [4,6–8,111]. Also the non-hydrolytic approach provides slower nanosilica growth, thus facilitating better structure and morphology control [8,112]. The first O–I polymer, with in situ generated silica domains, was prepared by Wilkes using TEOS and functionalized polymer [104]. The Wilkes morphological model described the O–I polymer as a hybrid network consisting of flexible polymer-rich domains with dispersed glassy silica-rich domains and a mixed interface. Since then, many in situ formed polymer–silica nanocomposites based on polypropylene (PP) [113–115], polyvinyl acetate (PVA) [116], polyvinyl alcohol (PVOH) [117–119], high amorphous vinyl alcohol (HAVOH) [11], polymethyl methacrylate (PMMA) [120], polydimethylsiloxane (PDMS) [121,122], polyacrylate [123,124] and epoxy matrix [4,7,112], were successfully synthesized.

Generally, the O–I polymer forms a complex structure and a multiphase morphology. The development of the phase structure plays an important role in the polymer hybrid build-up. During the O–I system polymerization the microphase separation takes place and the resulting hybrid structure and morphology depend on reaction conditions, system composition, diluent, etc. Physical interaction or covalent bonding between phases improves O–I system compatibility leading to the finer morphology, thus affects final nanocomposites' properties. The interfacial region starts at the nanoparticle's, where the properties differ from the bulk, and finishes at the polymer matrix boundaries, where the properties become equal to the matrix bulk. This region is between 2 nm and 50 nm thick, where its size depends on the nanofiller's dispersion, size and shape [98], and its chemical characteristics, crystallinity and polymer chain mobility can be altered from the bulk [125]. In order to increase interfacial bonding, and to obtain homogeneous dispersion, three main strategies are usually applied; (i) inorganic particles' surface modification, (ii) polymer matrices surface modification and (iii) interfacial modifier, compatibilizer or coupling agent application [107,109].

The silica surface modification with silane coupling agents ($\text{Si}(\text{OR})_3\text{R}'$) is one of the most often used techniques and can be performed in both aqueous and nonaqueous systems. These bifunctional agents contain two terminal functionally active groups, creating silica–polymer bonding, where the $\text{Si}(\text{OR})_3$ group reacts with silica and the functional organic group reacts/interacts with the polymer matrix. Triethoxyvinylsilane (VTS), 3-(Trimethoxysilyl)propyl methacrylate (MPTS), (3-Glycidyloxypropyl)trimethoxysilane (GTMS), (3-Aminopropyl)trimethoxysilane (APTS), (3-Mercaptopropyl)trimethoxysilane (McPTS) and (3-Chloropropyl)trimethoxysilane (CPTS) are some of the commonly used silane coupling agents [107].

Significant dispersion improvements could be obtained by Matějka et al. in epoxy–silica nanocomposites when Glycidyltrimethoxysilane (GTMS) was used as coupling agent in nonhydrolytic sol-gel process. The slow structure formation prevented phase separation improving homogeneity and, as a consequence, thermo–mechanical properties. The covalent interfacial adhesion significantly increased the storage moduli when compared to pure epoxy matrix [112]. Improvements in T_g and thermal stability of epoxy–silica nanocomposites were also obtained by nonhydrolytic sol-gel process with assistance of GTMS. Authors found out that the synergistic effect produced by the TEOS/TMOS/GTMS combination could further improve nanocomposites' thermo–mechanical performance. This approach allows better structure control during polymerization, resulting in easier tuning of hybrids morphology and final properties [126].

In the case of self-assembled systems, the noncovalent interactions are necessary to provide enough mobility to the molecules. In such systems, the application of non-reactive interfacial modifier or compatibilizer is a practical way for the silica dispersion improvement [107,109]. Ethyl methacrylate (EMA), ethylene ethyl acrylate (EEA) and ethyl butacrylate (EBA) copolymers as well sulfonate salts are some examples of frequently used compatibilizers and surfactants. These molecules do not form covalent bonding, but they are miscible and interact with nanocomposite components. Moreover,

the reversible nature of noncovalent interactions (e.g., H-bonding and ionic interactions) allows preparation of self-healing, stimuli-responsive and renewable materials.

5.1. Ionic Liquids as Multifunctional Additives in Polymer–Silica Nanocomposites

Initially, ILs were applied almost exclusively as a substitution of the conventional volatile organic solvents, transforming dangerous processes in recyclable and environmental friendly [42]. Later on, the range of application fields was broadened to the use in polymerization, electrolytes in batteries and in the nanocomposites preparation. Especially the ILs with imidazolium cation were applied in variety of processes and materials, principally due to their feasible property tuning via cation and anion structural modification and auto-organization characteristic [77]. Moreover, their further functionalization allows adaptation for better interaction in specific polymer systems (Figure 7). When ILs are present from the beginning of the sol-gel, where all the reagents are still molecularly distributed, small IL amounts may cause significant effects. Thus, applying ILs via sol-gel method into polymer matrices decrease the need of their removal at the end of the process. In this way, they act as compatibilizing, dispersing and lubricating agents, i.e., active multifunctional additives, improving nanocomposite physicochemical properties.

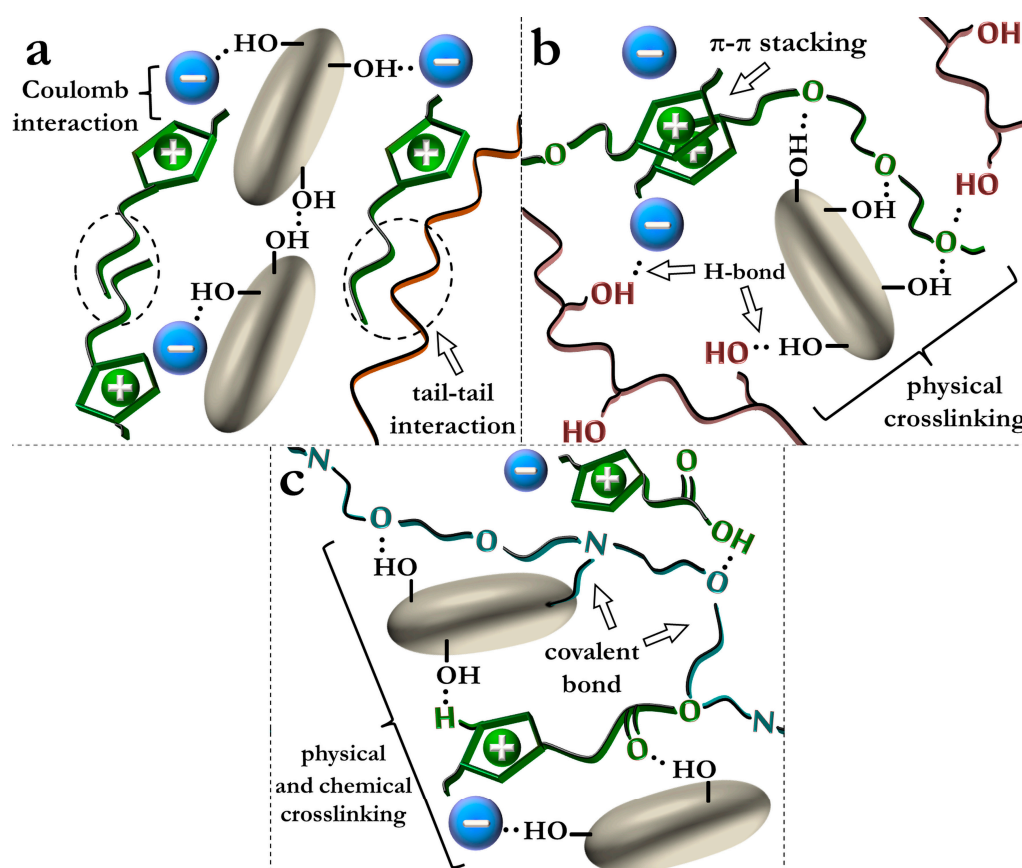


Figure 7. Representation types of interfacial interactions among silica-IL and (a) nonpolar (e.g., polyolefins) and polar (b) PVOH and (c) epoxy resins.

Considering the IL-silica modification to be applied into a polymer matrix, some studies should be mentioned; Donato et al. introduced IL-modified xerogel silica, containing imidazolium cations functionalized with long aliphatic chains (alkyl-IL), into melted iPP providing improvements in the dispersion and decrease in filler compactness. The synergism obtained due to silica/IL addition provoked an increase in the nanocomposites thermal resistance. The compatibilization between nonpolar matrix and polar filler (Figure 7a) was confirmed by increase in T_c , where the hybrid filler

worked as nucleating agent [6]. Carvalho et al. covalently bonded 1-(3-trimethoxysilylpropyl)-3-methylimidazolium chloride to the growing sol-gel silica, affecting the gelation time, surface area and morphology. Then, the IL modified-silica was compounded with epoxy prepolymer, affecting the rheological properties of the uncured dispersions and the glass transition temperature of the cured hybrid without influencing the storage modulus [127]. Detailed studies of IL-driven sol-gel mechanisms in epoxy–silica systems were performed by Perchacz et al. [10]. The structure of the obtained silica-IL precursors varied from highly condensed 3D cage-like, branched ladder-like to cyclic ones when C_4MImCl or $C_4MImMeSO_3$ were applied, respectively (Figure 8). An extensive experimental (^{29}Si NMR, rheology measurements, MALDI-TOF and ATR-FTIR spectroscopy) and theoretical (DFT) study demonstrated that precursor characteristics and evolution were driven mostly by H-bonding interactions between the imidazolium ring, the anion and the growing silicon species. Moreover, the authors found evidence that a kind of silanol/silicate transition could be happening in specific conditions, where the silicate anion formed could be stabilized by the positively charged imidazolium ring (Figure 8). The pre-formed silica-IL precursors incorporation into epoxy–amine matrix caused general nanocomposite thermal and mechanical reinforcement (e.g., ~50% increase in the energy to break and 40% increase in the elongation at break), where Silica- $C_4MImMeSO_3$ presented the best efficacy.

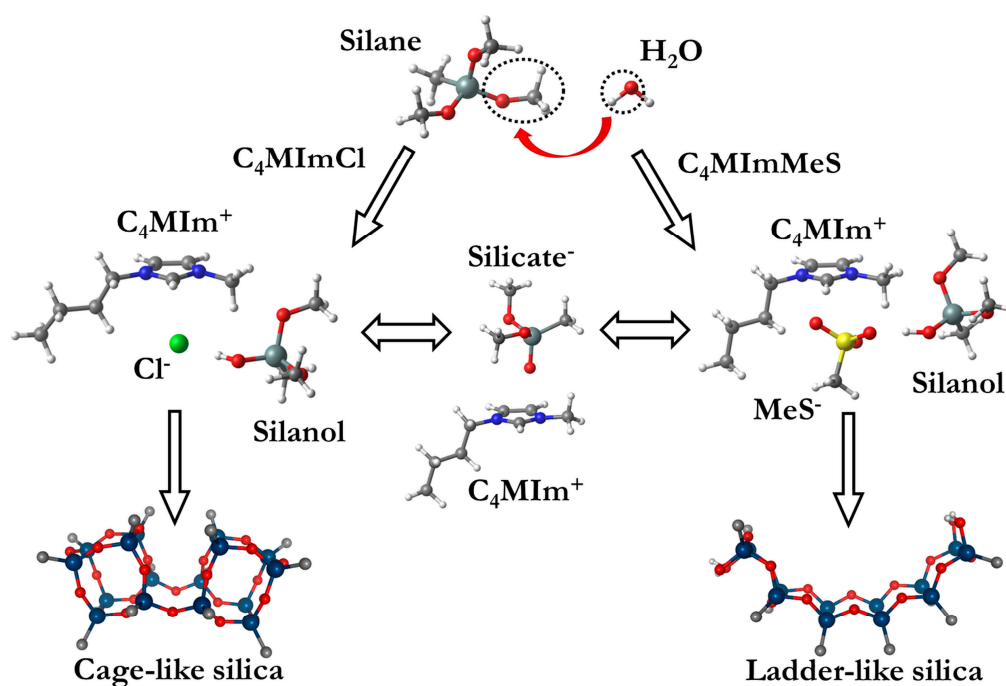


Figure 8. Theoretical structures and evolution of Silica-IL precursors when $[C_4MIm][Cl]$ or $[C_4MIm][MeSO_3]$ were applied [10] (permission obtained for reproduction).

The application of ILs into the two-step simultaneous filler-matrix polymerization, e.g., epoxy/sol-gel silica, allowed further improvement in nanofiller dispersion, since all components were in the liquid state (molecular level dispersion) during the mixing step. Moreover, these systems showed high sensibility to the type of IL applied, where alkyl-IL caused significant increase in the epoxy matrix brittleness and decreasing the toughness [4]. On the other hand, the addition of IL functionalized with ether (ether-IL) or carboxy (carboxy-IL) groups promoted not only an excellent nanosilica dispersion but also presented good filler-matrix interfacial interaction. This permitted preparation of nanocomposites with high storage modulus and tensile strength, as well as, with a high extensibility and toughness. The capacity of H-bonding, presented by ether-IL [32], and covalent

bonding, by carboxyl-IL, (Figure 7c) permitted interphase tuning and produced nanocomposites with high toughness without decrease in storage moduli [7,8].

Interestingly, most of the effects discussed herein happened exclusively when the ILs were applied into the sol-gel process or during the in situ simultaneous nanocomposite formation. Otherwise, when applied ex situ or as a simple additive/compatibilizer to nanocomposite formation ILs mainly produced plasticizing effects to the polymer matrix, especially in the case of melt compounding. Moreover, applying the ILs in the first steps of the sol-gel process or nanocomposite formation demanded only very small amounts of IL (<1 wt %) to cause drastic modifications into the systems. This demonstrated a multifunctional role of the ILs during both silica structuration and polymer matrix morphological evolution [4,6].

5.2. Applications of Polymer–Silica-IL Nanocomposites

The abovementioned multiple-bonding nature of the interfaces formed by ILs caused many interesting properties to be inherited by the host matrix. Especially properties that depend on this non-permanent or mobile interphase structure seem to be usually produced by those IL modifications. Moreover, there is an often misconception that as ILs produce interphases with physical bonding, i.e., H-bonding, van der Waals and Coulomb coupling, their contribution to the final properties are insignificant. However, especially the ions in these multi-ionic environments behave as distinct species rather than a simple ensemble of ions, forming complex multi-ion systems. Thus, differently from covalent bonds, these interactions can be present all over the interphase, affecting all the physical and chemical properties [128]. Although there has been a recent investigation topic and the literature produced is not very broad, initial results are quite promising in areas like; (i) gas/liquid barrier/selectivity properties, (ii) shape-memory materials and (iii) materials with self-healing properties.

5.2.1. IL-Based Nanocomposites with Barrier Properties

Controlled liquid and gas permeation is a well-desired property for materials applied to areas like smart packaging and membranes. The use of ILs and PILs for obtaining gas/liquid selective composite materials has already proven to be a feasible approach. The sum of their properties, i.e., thermal/chemical stability, low melting point, negligible vapor pressure and multiple bonding capacity, allows creating materials with permanent highly interactive liquid interphases, which can selectively interact with different gases/liquids depending on the IL's chemical structure [129,130] (Figure 9). This allowed preparing, e.g., IL-silica membrane, using a silylated IL, with superior separation factor of toluene/H₂ (>17,000) [131]; IL/PIL-based metal-organic frameworks (MOFs) that allow olefin/paraffin separation [132], in situ transform dienes into monoenes [133] or sense and actuate when in the presence of NH₃ [134]; or even a vast number of different supported-IL membranes, polymer/IL composite membranes, gelled IL membranes and PILs-based membranes for CO₂ separation [135].

Moreover, the application of ILs as sustainable alternatives to traditional cross-linkers, such as glutaraldehyde, often hazardous for health and environment, for water-soluble thermoplastic polymers was also proposed. Polyvinyl alcohol (PVOH)-silica nanocomposites, in the form of thin transparent films for packaging, coating or membrane applications, were prepared by in situ sol-gel method in the presence of alkyl-, ether- and carboxyl-ILs using aqueous PVOH solution. Due to the polar character of the matrix, both ether-ILs and carboxy-ILs paired with more coordinative anions (i.e., [Cl] or [MeSO₃]) formed stronger interfacial interactions, H-bond “physical cross-links” (Figure 7b), throughout the system causing significant improvements in water vapor barrier properties (~50%), storage modulus (~50%) and extensibility (~300%). This approach reduces the necessity of multilayer structuring with polyolefins, since it could be used as single-layer biodegradable film [11].

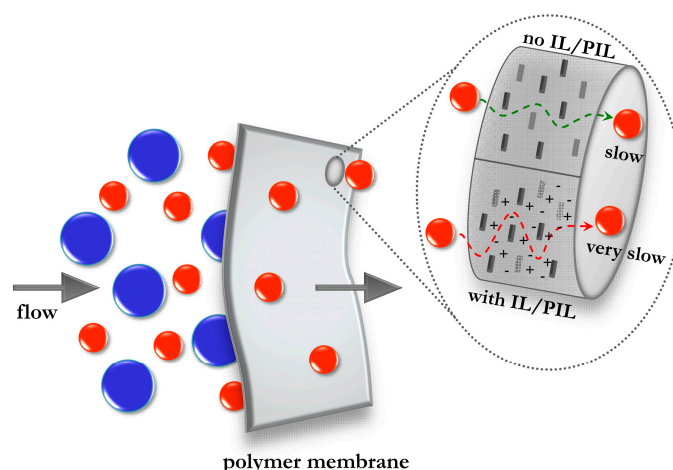


Figure 9. Schematic representation of the liquid/gas permeation through a polymer membrane. A slow flow is caused by the filler/polymer via tortuous path, where the addition of IL/PIL cause an even slower/more selective permeation due to their multiple-interaction features.

5.2.2. IL-Based Shape–Memory Materials

In the last decades, the attention of many researchers has been attracted by smart systems as materials responding to stimuli of an external environment. Shape–memory polymers (SMP) are special types of smart materials. They are stimuli-responsive polymers that can be deformed and fixed into a temporary shape and have the ability to recover the original, permanent shape upon exposure to an external stimulus, such as temperature, electric field and electromagnetic radiation.

In order to, e.g., thermally induce a shape–memory effect, the polymer is heated and deformed in the rubbery state. The deformed shape is then locked-in by cooling the material below the critical temperature T_C , corresponding to T_g to vitrify the system, or melting temperature to crystallize it in the case of a semicrystalline polymer. The shape fixing at low temperature is an important characteristic of SMP. The elastic energy is thus stored in the material. The subsequent system heating to an above T_C temperature leads to the shape recovery or to generation of the recovery stress under constrained conditions [136–138].

A common feature among different SPM based on polymer nanocomposites and blends is the presence of interphases dominated by physical interaction, such as van der Waals and ionic interactions, due to their mobile characteristic. Thus, shape-memory effect can be found in systems consisting of ionic interphases, such as, ionic polymers or PILs bearing host–guest interactions with small molecules [139] or with another polymer matrix [140], PIL-metal nanocomposites [141] and IL/PIL containing polymer-silica nanocomposites [9,142].

Dubois et al. converted a commercial polylactide (PLA) and endowed with shape-memory properties by forming an ionic nanocomposite network based on blends of PLA with imidazolium-terminated PLA and poly[ϵ -caprolactone-co-D,L-lactide] (P[CL-co-LA]) and surface-modified silica nanoparticles. The ionic hybrids were much more deformable compared to the neat PLA, also exhibiting shape–memory behavior with fixity ratio $R_f \approx 100\%$ and recovery ratio $R_r = 79\%$. The observed shape–memory behavior is a consequence of the ionic interactions preventing permanent slippage in the hybrids. The reversible and dynamic ionic bonding between the imidazolium-terminated polymers and the sulfonated silica nanoparticles led to distinct morphologies and very good nanoparticle dispersion within the hybrids. The sum of the improved morphology with an ionic polymer–filler interphase led to an exceptional performance, presenting an extremely long rubbery plateau and longer relaxation times, consistent with the significant shape–memory behavior observed [142].

Matějka et al. prepared a high performance SMP based on the epoxy–silica nanocomposites where the silica nanofiller was generated in situ within the epoxy matrix by the non-aqueous sol-gel process [9]. The shape memory properties, such as recovery stress, shape fixity and completeness of shape recovery, as well as the efficiency of the SMP to store the elastic energy, were improved by applying a very small amount (0.2 wt %) of IL, namely $[C_4MIm][BF_4]$, $[C_{10}MIm][BF_4]$ and $[C_4MIm][Cl]$, into the epoxy–silica hybrid synthesis. The nanocomposites presented a dual shape–memory effect, where part of the shape was recovered at 60 °C and the complete recovery happened at 100 °C (Figure 10). The IL application also enhanced rubbery modulus and significantly increased toughness of the hybrids due to the strong physical dynamic interphase interaction undergoing a breaking–formation process. As a result, the recovery stress is significantly increased because of its close correlation with material toughness. Moreover, due to the modification of the epoxy–silica interphase, the IL improved the nanocomposite homogeneity, thereby reducing broadness of the T_g and the polymer viscoelasticity effect. Consequently, the loss of stored mechanical energy by polymer relaxation during the shape–memory cycle (heating–cooling–heating) is reduced and the efficiency of the SMP is increased. The synthesized epoxy–silica hybrids showed excellent shape fixity ($\sim 100\%$), complete recovery ($>98\%$) and very high recovery stress, $\sigma_r = 3.9$ MPa [9].

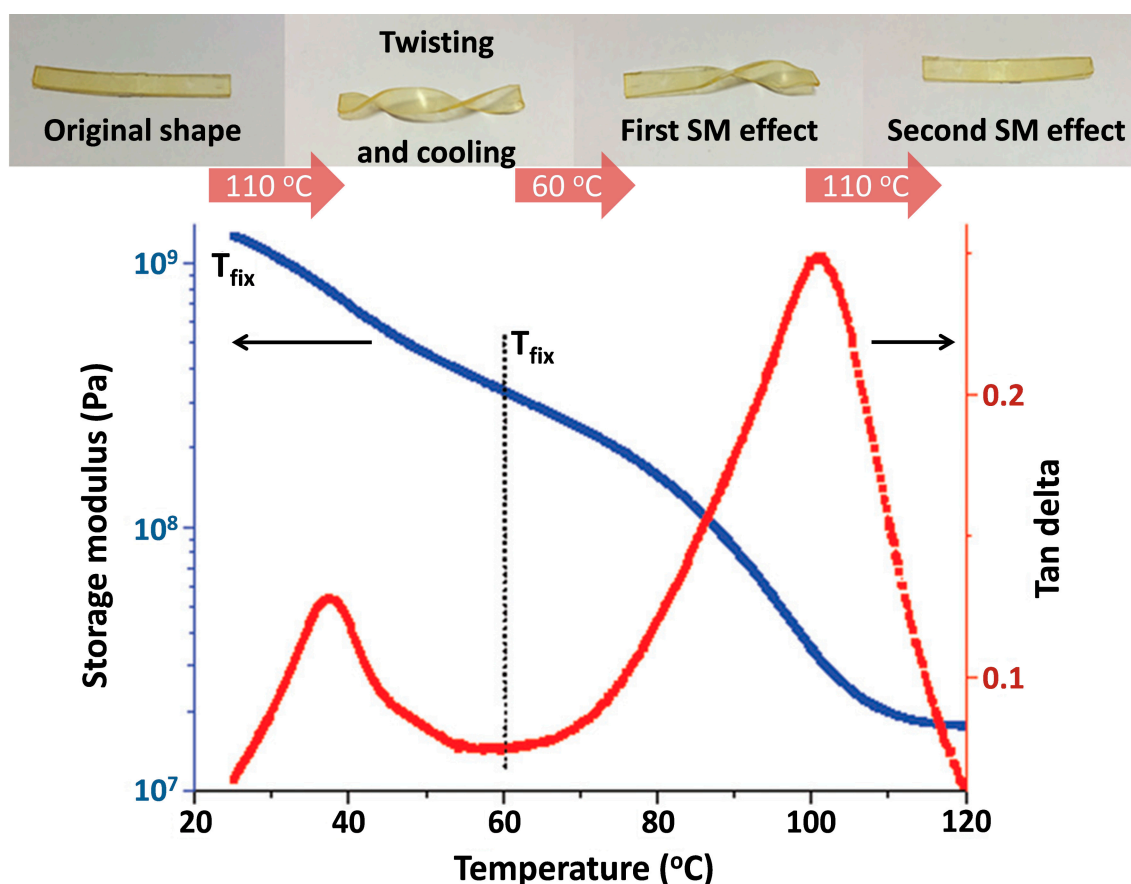


Figure 10. Images from an epoxy–silica-IL nanocomposite with dual SM effect showing its initial shape, deformation after heating up to 110 °C and subsequent cooling down, and first (60 °C) and second (110 °C) stages of SM effect (above). Nanocomposite's storage modulus and loss factor $\tan \delta$ temperature sweep, showing the transitions related to the dual SM effect [9] (Reproduced from Ref. [9] with permission from The Royal Society of Chemistry.).

5.2.3. IL-Based Self-Healing Materials

The self-healing polymer materials belong to the most promising applications of a smart behavior. These polymers are stimuli responsive and possess the ability to self-heal when damaged [143–145]. Often inspired by nature-based materials, synthetic self-healing allows the preparation of multifunctional materials that recover their fundamental properties, including mechanical strength, conductivity, fracture toughness, and corrosion resistance, after damage infliction. Although the usefulness and practicality of these materials, when considering the field of polymer nanocomposites, self-healing has remained unexplored up to very recently, providing a broad field of opportunities to be explored [146].

Just to name a few; a SMP assisted self-healing has been reported [147], consisting of the combination of two processes in a single heating step, the so called close-then-heal scheme [148]. The SMP effect results in closing microcracks in a damaged material, and rebonding by the reversible cross-linking leads then to healing nanoscopic deterioration, such as chain scission. Another approach demonstrated was the formation of silica nanocontainers loaded with, e.g., a corrosion inhibitor 2-mercaptobenzothiazole in a hybrid sol-gel, obtaining polymer–silica nanocontainers for self-healing coatings with enhanced corrosion protection activity [149].

An often common feature of such materials is the presence of dynamic interactions, such as multiple H-bonding, hydrophobic interactions, π - π stacking, metal–ligand coordination and ionic bonding. However, up to very recently the role of ionic bonding in the healing mechanism was unknown. Some light was shone upon this subject when Kalista Jr. et al. demonstrated the significant role of ionicity in the polymer healing process. They observed that, especially at lower temperatures, non-ionic materials lack sufficient strength around the crack site, which is a pre-requisite for maintaining a rigid framework during local elastic recovery. However, they also observed that highly ionic materials are only beneficial for temperatures increasing into the melt, while moderately ionic materials exhibited the best healing response over a broad temperature range [150]. These observations lead to the conclusion that materials presenting ionicity in their interfaces tend to have improved self-healing characteristics, but also that purely ionic interfaces are not the ideal approach. Based on that, the use of ILs or PILs as one of the system's components provides that ionicity necessary for an effective healing interphase.

Based on this idea, the use of ILs/PILs was demonstrated in many different polymer systems, such as: block copolymer/IL-based functional soft materials presenting spontaneous repair damage by light illumination, driven by a reversible gel-sol-gel transition cycle with a reversible association/fragmentation of the polymer network [151]; IL-modified epoxy resin thermoset with self-healing ability for surface abrasion damage, where the viscoelastic recovery and healing ability of the damaged surface increases with increasing IL content (up to ~12 wt %) [152]; polymer/IL-based transparent, self-healing, highly stretchable ionic conductor, used to electrically activate transparent artificial muscles, that autonomously heals using ion–dipole interactions as the dynamic motif [153]; ionically cross-linked poly(acrylic acid) (PAA) and poly-(triethyl(4-vinylbenzyl)phosphonium chloride) networks presenting a salinity dependent swelling behavior, allowing them to self-heal in low and physiologically relevant salt concentrations for biomedical area [154]; or converting bromobutyl rubber into ionic imidazolium bromide reversible ionic associates, presenting physical cross-linking ability, which facilitates the healing processes by temperature- or stress-induced rearrangements, thereby enabling a fully cut sample to retain its original properties after the self-healing process [155]; just to mention a few.

However, the implementation of self-healing structures into a polymer generally leads to a decrease in mechanical properties of a material. Thus, new approaches are necessary to overcome this drawback. The epoxy–silica hybrids synthesized in the presence of ILs proved to be efficient as high performance SMP [9], which work with similar dynamic bonding mechanisms as self-healing materials, but preserving or even improving the original mechanical properties of the polymer matrix. This could be demonstrated by Dubois et al., which synthesized ionic nanocomposites based

on imidazolium-functionalized polyurethanes and surface-modified sulfonated silica nanoparticles forming an extensive 3D network of well-dispersed particles. Consequently, mechanical improvements such as 11-fold increase in strain at break, 40-fold increase in tensile toughness and a 2.5-fold increase in stiffness, compared to the neat polymer, could be obtained. The dynamic and reversible nature of the ionic crosslinks within the nanocomposites inflicts remarkable reversible plasticity/shape-recovery. This gives the nanocomposites a unique strain-dependent behavior, where the deformation increases with increasing strain rate, and return to the normal state after deformation, including both shape-memory and self-healing properties [156] (Figure 11).

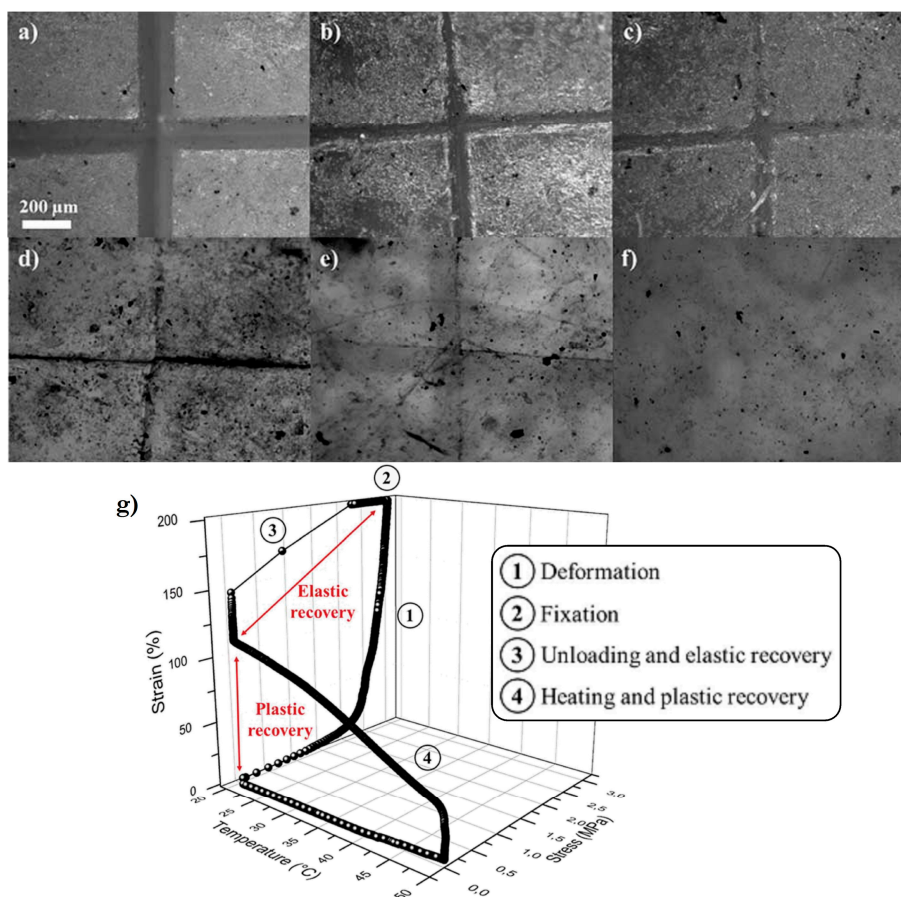


Figure 11. Microscopic images of the nanocomposites immediately after a scratch damage was inferred (a); and after being held at 50 °C for 1 h (b); 2 h (c); 3 h (d); 4 h (e) and 5 h (f); demonstrating the self-healing behavior. Cyclic stress-controlled thermomechanical test of the nanocomposite showing reversible plasticity/shape-memory (g) [156] (Reprinted from Ref. [156] with permission of The Royal Society of Chemistry.).

6. Conclusions and Outlook

This review discussed the application of ionic liquids (ILs) and poly ionic liquids (PILs) to nanocomposite formation, their effects during the processes and in the final composites properties, highlighting their interfacial effects, especially when colloidal processes were involved. As a background for the discussion, the state-of-art of the following subjects was covered: (i) hybrid formation using the sol-gel process; (ii) molecular imprinting during the sol-gel process; (iii) the ILs and their role when applied into the sol-gel process; (iv) molecular imprinting of ILs into sol-gel species, also within complex systems (ex situ and in situ) such as polymer matrices; (v) the ILs'

multiple-bonding nature effects at the materials interfaces; and (vi) the applications that may emerge from this strategies.

The application of ILs into the sol-gel process allows structural control, conducted by their self-assembly and multiple-bonding features. ILs interact with the growing system through H-bond “co- π - π stacking” mechanism, forming a variety of morphologically different hybrid materials under mild reaction conditions. This creates an ordered solvation layer of ILs on the silica surface, which influences the interfacial interactions. Thus, differences in size, geometry, polarity and Coulomb coupling forces between cations and anions, which influence ILs’ viscosity and transition temperatures, directly contribute to the final silica particles morphology, size and compactness. Moreover, the presence of the C-H unities in the imidazolium ring and functionalization with polar groups could further intensify the ILs multiple H-bonding.

These ILs’ features significantly influence the nanocomposites/hybrids interfaces, also adding to them an ionic character. However, not many studies discuss the interface ionicity influence to the nanocomposites properties. Only very recently, this subject has been raised and very promising results were observed. Besides the outstanding mechanical properties reinforcements, very desirable properties, such as selective gas/liquid permeability, shape-memory and self-healing, were added to the final nanocomposites. Thus, we hope to have convinced researchers, especially from the areas of colloidal and interface sciences, that further investigations in this subject are worthwhile and could allow developing prospective new materials for many areas, such as biomedicine, electronics, aerospace, smart fabrics, intelligent packaging, sensors and actuators.

Acknowledgments: The authors thank the Brazilian funding agencies CNPq, CAPES and FAPERGS for financial support. This work was also partially supported by the EU H’2020-MSCA-RISE-734164 Graphene 3D project. RKD acknowledge FAPESP (SPEC Project 2012/50259-8) for financial support.

Author Contributions: R.S.M. and L.M. gave support on the scientific discussions and revised the paper. K.Z.D. and R.K.D. prepared the artwork, revised the literature and wrote the paper.

Conflicts of Interest: The authors declare no conflict of interest.

References

1. Sanchez, C.; Belleville, P.; Popall, M.; Nicole, L. Applications of advanced hybrid organic–inorganic nanomaterials: From laboratory to market. *Chem. Soc. Rev.* **2011**, *40*, 696. [[CrossRef](#)] [[PubMed](#)]
2. Brinker, C.J.; Scherer, G.W. *Sol-Gel Science: The Physics and Chemistry of Sol-Gel Processing*; Elsevier: Amsterdam, The Netherlands, 1990; ISBN 9780121349707.
3. Donato, R.K.; Lavorgna, M.; Musto, P.; Donato, K.Z.; Jager, A.; Štěpánek, P.; Schrekker, H.S.; Matějka, L. The role of ether-functionalized ionic liquids in the sol-gel process: Effects on the initial alkoxide hydrolysis steps. *J. Colloid Interface Sci.* **2015**, *447*, 77–84. [[CrossRef](#)] [[PubMed](#)]
4. Donato, R.K.; Matějka, L.; Schrekker, H.S.; Pleštil, J.; Jigounov, A.; Brus, J.; Šlouf, M. The multifunctional role of ionic liquids in the formation of epoxy-silica nanocomposites. *J. Mater. Chem.* **2011**, *21*, 13801. [[CrossRef](#)]
5. Donato, K.Z.; Donato, R.K.; Lavorgna, M.; Ambrosio, L.; Matějka, L.; Mauler, R.S.; Schrekker, H.S. Ionic liquids as dynamic templating agents for sol-gel silica systems: Synergistic anion and cation effect on the silica structured growth. *J. Sol-Gel Sci. Technol.* **2015**, *76*, 414–427. [[CrossRef](#)]
6. Donato, R.K.; Benvegnú, M.A.; Furlan, L.G.; Mauler, R.S.; Schrekker, H.S. Imidazolium salts as liquid coupling agents for the preparation of polypropylene-silica composites. *J. Appl. Polym. Sci.* **2010**, *116*, 304–307. [[CrossRef](#)]
7. Donato, R.K.; Donato, K.Z.; Schrekker, H.S.; Matějka, L. Tunable reinforcement of epoxy-silica nanocomposites with ionic liquids. *J. Mater. Chem.* **2012**, *22*, 9939. [[CrossRef](#)]
8. Donato, R.K.; Perchacz, M.; Ponyrko, S.; Donato, K.Z.; Schrekker, H.S.; Beneš, H.; Matějka, L. Epoxy-silica nanocomposite interphase control using task-specific ionic liquids via hydrolytic and non-hydrolytic sol-gel processes. *R. Soc. Chem. Adv.* **2015**, *5*, 91330–91339. [[CrossRef](#)]
9. Ponyrko, S.; Donato, R.K.; Matějka, L. Tailored high performance shape memory epoxy-silica nanocomposites. Structure design. *Polym. Chem.* **2016**, *7*, 560–572. [[CrossRef](#)]

10. Perchacz, M.; Donato, R.K.; Seixas, L.; Zhigunov, A.; Serkis-rodzen, M.; Benes, H. Ionic Liquid-Silica Precursors via Solvent-Free Sol–Gel Process and Their Application in Epoxy-Amine Network: A Theoretical/Experimental Study. *ACS Appl. Mater. Interfaces* **2017**, *9*, 16474–16487. [[CrossRef](#)] [[PubMed](#)]
11. Donato, K.Z.; Lavorgna, M.; Donato, R.K.; Raucci, M.G.; Buonocore, G.G.; Ambrosio, L.; Schrekker, H.S.; Mauler, R.S. High Amorphous Vinyl Alcohol-Silica Bionanocomposites: Tuning Interface Interactions with Ionic Liquids. *ACS Sustain. Chem. Eng.* **2017**, *5*, 1094–1105. [[CrossRef](#)]
12. Danks, A.E.; Hall, S.R.; Schnepf, Z. The evolution of “sol-gel” chemistry as a technique for materials synthesis. *Mater. Horiz.* **2016**, *3*, 91–112. [[CrossRef](#)]
13. Pagliaro, M.; Ciriminna, R.; Palmisano, G. Silica-based hybrid coatings. *J. Mater. Chem.* **2009**, *19*, 3116. [[CrossRef](#)]
14. Nassif, N.; Livage, J. From diatoms to silica-based biohybrids. *Chem. Soc. Rev.* **2011**, *40*, 849–859. [[CrossRef](#)] [[PubMed](#)]
15. Vallet-Regí, M.; Colilla, M.; González, B. Medical applications of organic–inorganic hybrid materials within the field of silica-based bioceramics. *Chem. Soc. Rev.* **2011**, *40*, 596–607. [[CrossRef](#)] [[PubMed](#)]
16. Letailleur, A.A.; Ribot, F.; Boissière, C.; Teisseire, J.; Barthel, E.; Desmazières, B.; Chemin, N.; Sanchez, C. Sol-gel derived hybrid thin films: The chemistry behind processing. *Chem. Mater.* **2011**, *23*, 5082–5089. [[CrossRef](#)]
17. Sanchez, C.; Shea, K.J.; Kitagawa, S. Recent progress in hybrid materials science. *Chem. Soc. Rev.* **2011**, *40*, 471–472. [[CrossRef](#)] [[PubMed](#)]
18. Avnir, D.; Levy, D.; Reisfeld, R. The nature of the silica cage as reflected by spectral changes and enhanced photostability of trapped Rhodamine 6G. *J. Phys. Chem.* **1984**, *88*, 5956–5959. [[CrossRef](#)]
19. Kaufman, V.R.; Levy, D.; Avnir, D. A photophysical study of the sol/gel transition in silica: Structural dynamics and oscillations, room-temperature phosphorescence and photochromic gel glasses. *J. Non-Cryst. Solids* **1986**, *82*, 103–109. [[CrossRef](#)]
20. Owens, G.J.; Singh, R.K.; Foroutan, F.; Alqaysi, M.; Han, C.M.; Mahapatra, C.; Kim, H.W.; Knowles, J.C. Sol-gel based materials for biomedical applications. *Prog. Mater. Sci.* **2016**, *77*, 1–79. [[CrossRef](#)]
21. Tang, S.; Liu, S.; Ren, H.; Liang, X.; Qiu, H.; Guo, Y.; Liu, X.; Jiang, S. A novel imidazolium-based organic–silica hybrid monolith for per aqueous capillary electrochromatography. *R. Soc. Chem. Adv.* **2014**, *4*, 25819. [[CrossRef](#)]
22. Hallett, J.P.; Welton, T. Room-Temperature Ionic Liquids: Solvents for Synthesis and Catalysis. 2. *Chem. Rev.* **2011**, *111*, 3508–3576. [[CrossRef](#)] [[PubMed](#)]
23. Maton, C.; De Vos, N.; Stevens, C.V. Ionic liquid thermal stabilities: Decomposition mechanisms and analysis tools. *Chem. Soc. Rev.* **2013**, *42*, 5963–5977. [[CrossRef](#)] [[PubMed](#)]
24. Zhang, S.; Sun, N.; He, X.; Lu, X.; Zhang, X. Physical Properties of Ionic Liquids: Database and Evaluation. *J. Phys. Chem. Ref. Data* **2006**, *35*, 1475–1517. [[CrossRef](#)]
25. Gabriel, S.; Weiner, J. Ueber einige Abkömmlinge des Propylamins. *Eur. J. Inorg. Chem.* **1888**, *21*, 2669–2679. [[CrossRef](#)]
26. Walden, P. Molecular weights and electrical conductivity of several fused salts. *Bull. Acad. Imper. Sci.* **1914**, *8*, 405–422.
27. Hurley, F.H.; Wier, T.P. The Electrodeposition of Aluminum from Nonaqueous Solutions at Room Temperature. *J. Electrochem. Soc.* **1951**, *98*, 207. [[CrossRef](#)]
28. Işık, M.; Sardon, H.; Mecerreyes, D. Ionic Liquid and Cellulose Technologies: Dissolution, Modification and Composite Preparation. In *Applications of Ionic Liquids in Polymer Science and Technology*; Springer: Berlin/Heidelberg, Germany, 2015; pp. 135–152.
29. Dupont, J.; Suarez, P.A.Z. Physico-chemical processes in imidazolium ionic liquids. *Phys. Chem. Chem. Phys.* **2006**, *8*, 2441. [[CrossRef](#)] [[PubMed](#)]
30. Tang, S.; Baker, G.A.; Zhao, H. Ether- and alcohol-functionalized task-specific ionic liquids: Attractive properties and applications. *Chem. Soc. Rev.* **2012**, *41*, 4030–4066. [[CrossRef](#)] [[PubMed](#)]
31. Chen, Z.J.; Xue, T.; Lee, J.-M. What causes the low viscosity of ether-functionalized ionic liquids? Its dependence on the increase of free volume. *R. Soc. Chem. Adv.* **2012**, *2*, 10564–10574. [[CrossRef](#)]
32. Hunt, P.A.; Ashworth, C.R.; Matthews, R.P. Hydrogen bonding in ionic liquids. *Chem. Soc. Rev.* **2015**, *44*, 1257–1288. [[CrossRef](#)] [[PubMed](#)]

33. Schrekker, H.S.; Silva, D.O.; Gelesky, M.A.; Stracke, M.P.; Schrekker, C.M.L.; Gonçalves, R.S.; Dupont, J. Preparation, cation-anion interactions and physicochemical properties of ether-functionalized imidazolium ionic liquids. *J. Braz. Chem. Soc.* **2008**, *19*, 426–433. [[CrossRef](#)]
34. Zhou, Z.-B.; Matsumoto, H.; Tatsumi, K. Low-Melting, Low-Viscous, Hydrophobic Ionic Liquids: Aliphatic Quaternary Ammonium Salts with Perfluoroalkyltrifluoroborates. *Chem. A Eur. J.* **2005**, *11*, 752–766. [[CrossRef](#)] [[PubMed](#)]
35. Smith, G.D.; Borodin, O.; Li, L.; Kim, H.; Liu, Q.; Bara, J.E.; Gin, D.L.; Nobel, R. A comparison of ether- and alkyl-derivatized imidazolium-based room-temperature ionic liquids: A molecular dynamics simulation study. *Phys. Chem. Chem. Phys.* **2008**, *10*, 6301–6312. [[CrossRef](#)] [[PubMed](#)]
36. Fei, Z.; Ang, W.H.; Zhao, D.; Scopelliti, R.; Zvereva, E.E.; Katsyuba, S.A.; Dyson, P.J. Revisiting ether-derivatized imidazolium-based ionic liquids. *J. Phys. Chem. B* **2007**, *111*, 10095–10108. [[CrossRef](#)] [[PubMed](#)]
37. Bergamo, V.Z.; Donato, R.K.; Dalla Lana, D.F.; Donato, K.J.Z.; Ortega, G.G.; Schrekker, H.S.; Fuentefria, A.M. Imidazolium salts as antifungal agents: Strong antibiofilm activity against multidrug-resistant *Candida tropicalis* isolates. *Letts. Appl. Microbiol.* **2015**, *60*, 66–71. [[CrossRef](#)] [[PubMed](#)]
38. Schrekker, H.S.; Donato, R.K.; Fuentefria, A.M.; Bergamo, V.; Oliveira, L.F.; Machado, M.M. Imidazolium salts as antifungal agents: Activity against emerging yeast pathogens, without human leukocyte toxicity. *Medchemcomm* **2013**, *4*, 1457. [[CrossRef](#)]
39. Pendleton, J.N.; Gilmore, B.F. The antimicrobial potential of ionic liquids: A source of chemical diversity for infection and biofilm control. *Int. J. Antimicrob. Agents* **2015**, *46*, 131–139. [[CrossRef](#)] [[PubMed](#)]
40. Riduan, S.N.; Zhang, Y. Imidazolium salts and their polymeric materials for biological applications. *Chem. Soc. Rev.* **2013**, *42*, 9055–9070. [[CrossRef](#)] [[PubMed](#)]
41. Cui, B.; Zheng, B.L.; He, K.; Zheng, Q.Y. Imidazole alkaloids from *Lepidium meyenii*. *J. Nat. Prod.* **2003**, *66*, 1101–1103. [[CrossRef](#)] [[PubMed](#)]
42. Jordan, A.; Gathergood, N. Biodegradation of ionic liquids—A critical review. *Chem. Soc. Rev.* **2015**, *44*, 8200–8237. [[CrossRef](#)] [[PubMed](#)]
43. Mohammad, A.; Inamuddin, D. (Eds.) *Green Solvents II: Properties and Applications of Ionic Liquids*; Springer: Dordrecht, The Netherlands, 2012; ISBN 9789400728912.
44. Vijayaraghavan, R.; MacFarlane, D.R. Living cationic polymerisation of styrene in an ionic liquid. *Chem. Commun.* **2004**, *34*, 700–701. [[CrossRef](#)] [[PubMed](#)]
45. Perrier, S.; Davis, T.P.; Carmichael, A.J.; Haddleton, D.M. First report of reversible addition–fragmentation chain transfer (RAFT) polymerisation in room temperature ionic liquids. *Chem. Commun.* **2002**, *101*, 2226–2227. [[CrossRef](#)]
46. Shen, Y.; Tang, H.; Ding, S. Catalyst separation in atom transfer radical polymerization. *Prog. Polym. Sci.* **2004**, *29*, 1053–1078. [[CrossRef](#)]
47. Sarbu, T.; Matyjaszewski, K. ATRP of methyl methacrylate in the presence of ionic liquids with ferrous and cuprous anions. *Macromol. Chem. Phys.* **2001**, *202*, 3379–3391. [[CrossRef](#)]
48. Zhang, H.; Hong, K.; Mays, J.W. Synthesis of block copolymers of styrene and methyl methacrylate by conventional free radical polymerization in room temperature ionic liquids. *Macromolecules* **2002**, *35*, 5738–5741. [[CrossRef](#)]
49. Hanyu, Y.; Honma, I. Rechargeable quasi-solid state lithium battery with organic crystalline cathode. *Sci. Rep.* **2012**, *2*, 453. [[CrossRef](#)] [[PubMed](#)]
50. Ito, S.; Unemoto, A.; Ogawa, H.; Tomai, T.; Honma, I. Application of quasi-solid-state silica nanoparticles–ionic liquid composite electrolytes to all-solid-state lithium secondary battery. *J. Power Sources* **2012**, *208*, 271–275. [[CrossRef](#)]
51. Wang, P.; Zakeeruddin, S.M.; Comte, P.; Exnar, I.; Grätzel, M. Gelation of ionic liquid-based electrolytes with silica nanoparticles for quasi-solid-state dye-sensitized solar cells. *J. Am. Chem. Soc.* **2003**, *125*, 1166–1167. [[CrossRef](#)] [[PubMed](#)]
52. Kubo, W.; Kitamura, T.; Hanabusa, K.; Wada, Y.; Yanagida, S. Quasi-solid-state dye-sensitized solar cells using room temperature molten salts and a low molecular weight gelator. *Chem. Commun.* **2002**, *115*, 374–375. [[CrossRef](#)]

53. Fukushima, T.; Kosaka, A.; Ishimura, Y.; Yamamoto, T.; Takigawa, T.; Ishii, N.; Aida, T. Molecular ordering of organic molten salts triggered by single-walled carbon nanotubes. *Science* **2003**, *300*, 2072–2074. [[CrossRef](#)] [[PubMed](#)]
54. Lodge, T.P. A Unique Platform for Materials Design. *Science* **2008**, *321*, 50–51. [[CrossRef](#)] [[PubMed](#)]
55. Texter, J. Ionic liquids and polymeric ionic liquids as stimuli-responsive functional materials. In *Applications of Ionic Liquids in Polymer Science and Technology*; Springer: Berlin/Heidelberg, Germany, 2015; pp. 103–134, ISBN 9783662449035.
56. Klingshim, M.A.; Spear, S.K.; Subramanian, R.; Holbrey, J.D.; Huddleston, J.G.; Rogers, R.D. Gelation of Ionic Liquids Using a Cross-Linked Poly(Ethylene Glycol) Gel Matrix. *Chem. Mater.* **2004**, *16*, 3091–3097. [[CrossRef](#)]
57. Yuan, J.; Antonietti, M. Poly(ionic liquid)s as ionic liquid-based innovative polyelectrolytes. In *Applications of Ionic Liquids in Polymer Science and Technology*; Springer: Berlin/Heidelberg, Germany, 2015; pp. 47–67, ISBN 9783662449035.
58. Livi, S.; Gérard, J.-F.; Duchet-Rumeau, J. Ionic Liquids as Polymer Additives. In *Applications of Ionic Liquids in Polymer Science and Technology*; Springer: Berlin/Heidelberg, Germany, 2015; pp. 1–21, ISBN 978-3-662-44903-5.
59. Cai, M.; Liang, Y.; Zhou, F.; Liu, W. Ionic Liquids as Lubricants. In *Green Solvents II*; Springer: Dordrecht, The Netherlands, 2012; pp. 203–233.
60. Donato, R.K.; Migliorini, M.V.; Benvegnu, M.A.; Stracke, M.P.; Gelesky, M.A.; Pavan, F.A.; Schrekker, C.M.L.; Benvenuti, E.V.; Dupont, J.; Schrekker, H.S. Synthesis of silica xerogels with highly distinct morphologies in the presence of imidazolium ionic liquids. *J. Sol-Gel Sci. Technol.* **2009**, *49*, 71–77. [[CrossRef](#)]
61. Zhou, Y.; Schattka, J.H.; Antonietti, M. Room-temperature ionic liquids as template to monolithic mesoporous silica with wormlike pores via a sol-gel nanocasting technique. *Nano Lett.* **2004**, *4*, 477–481. [[CrossRef](#)]
62. Zhou, Y.; Antonietti, M. Preparation of highly ordered monolithic super-microporous lamellar silica with a room-temperature ionic liquid as template via the nanocasting technique. *Adv. Mater.* **2003**, *15*, 1452–1455. [[CrossRef](#)]
63. Zhou, Y.; Antonietti, M. A novel tailored bimodal porous silica with well-defined inverse opal microstructure and super-microporous lamellar nanostructure. *Chem. Commun.* **2003**, *206*, 2564–2565. [[CrossRef](#)]
64. Zhou, Y.; Antonietti, M. A Series of Highly Ordered, Super-Microporous, Lamellar Silicas Prepared by Nanocasting with Ionic Liquids. *Chem. Mater.* **2004**, *16*, 544–550. [[CrossRef](#)]
65. Adams, C.J.; Bradley, A.E.; Seddon, K.R. The Synthesis of Mesoporous Materials Using Novel Ionic Liquid Templates in Water. *Aust. J. Chem.* **2002**, *54*, 679–681. [[CrossRef](#)]
66. Le Bideau, J.; Viau, L.; Vioux, A. Ionogels, ionic liquid based hybrid materials. *Chem. Soc. Rev.* **2011**, *40*, 907–925. [[CrossRef](#)] [[PubMed](#)]
67. Cooper, E.R.; Andrews, C.D.; Wheatley, P.S.; Webb, P.B.; Wormald, P.; Morris, R.E. Ionic liquids and eutectic mixtures as solvent and template in synthesis of zeolite analogues. *Nature* **2004**, *430*, 1012–1016. [[CrossRef](#)] [[PubMed](#)]
68. Lu, A.H.; Schüth, F. Nanocasting: A versatile strategy for creating nanostructured porous materials. *Adv. Mater.* **2006**, *18*, 1793–1805. [[CrossRef](#)]
69. Jiang, P.; Bertone, J.F.; Colvin, V.L. A Lost-Wax Approach to Monodisperse Colloids and Their Crystals. *Science* **2001**, *291*, 453–457. [[CrossRef](#)] [[PubMed](#)]
70. Díaz-García, M.E.; Laíñ, R.B. Molecular Imprinting in Sol-Gel Materials: Recent Developments and Applications. *Microchim. Acta* **2005**, *149*, 19–36. [[CrossRef](#)]
71. Chen, L.; Wang, X.; Lu, W.; Wu, X.; Li, J. Molecular imprinting: Perspectives and applications. *Chem. Soc. Rev.* **2016**, *45*, 2137–2211. [[CrossRef](#)] [[PubMed](#)]
72. Dhainaut, J.; Dacquin, J.P.; Lee, A.F.; Wilson, K. Hierarchical macroporous-mesoporous SBA-15 sulfonic acid catalysts for biodiesel synthesis. *Green Chem.* **2010**, *12*, 296–303. [[CrossRef](#)]
73. Guan, Z.S.; Lu, C.H.; Zhang, Y.; Zi, X.Z. Morphology-controlled Synthesis of SiO₂ Hierarchical Structures Using Pollen Grains as Templates. *Chin. J. Chem.* **2008**, *26*, 467–470. [[CrossRef](#)]
74. Marx, S.; Avnir, D. The induction of chirality in sol-gel materials. *Acc. Chem. Res.* **2007**, *40*, 768–776. [[CrossRef](#)] [[PubMed](#)]
75. Fireman-Shoresh, S.; Avnir, D.; Marx, S. General method for chiral imprinting of sol-gel thin films exhibiting enantioselectivity. *Chem. Mater.* **2003**, *15*, 3607–3613. [[CrossRef](#)]

76. Huo, H.; Wang, S.; Lin, S.; Li, Y.; Li, B.; Yang, Y. Chiral zirconia nanotubes prepared through a sol-gel transcription approach. *J. Mater. Chem. A* **2014**, *2*, 333–338. [[CrossRef](#)]
77. Dupont, J. On the solid, liquid and solution structural organization of imidazolium ionic liquids. *J. Braz. Chem. Soc.* **2004**, *15*, 341–350. [[CrossRef](#)]
78. Dai, S.; Ju, Y.H.; Gao, H.J.; Lin, J.S.; Pennycook, S.J.; Barnes, C.E. Preparation of silica aerogel using ionic liquids as solvents. *Chem. Commun.* **2000**, *37*, 243–244. [[CrossRef](#)]
79. Xu, C.; Tang, R.; Hua, Y.; Zhang, P. Mesoporous Silica Materials Synthesized via Sol-Gel Methods Modified with Ionic Liquid and Surfactant Molecules Mesoporous Silica Materials Synthesized via Sol-Gel Methods Modified with Ionic Liquid and Surfactant Molecules. *Chin. J. Chem. Phys.* **2008**, *21*, 596–600. [[CrossRef](#)]
80. Karout, A.; Pierre, A.C. Silica xerogels and aerogels synthesized with ionic liquids. *J. Non-Cryst. Solids* **2007**, *353*, 2900–2909. [[CrossRef](#)]
81. Klingshirn, M.A.; Spear, S.K.; Holbrey, J.D.; Rogers, R.D. Ionic liquids as solvent and solvent additives for the synthesis of sol-gel materials. *J. Mater. Chem.* **2005**, *15*, 5174–5180. [[CrossRef](#)]
82. Kinoshita, K.; Yanagimoto, H.; Suzuki, T.; Minami, H. Influence of the molecular-oriented structure of ionic liquids on the crystallinity of aluminum hydroxide prepared by a sol-gel process in ionic liquids. *Phys. Chem. Chem. Phys.* **2015**, *17*, 18705–18709. [[CrossRef](#)] [[PubMed](#)]
83. Zhou, Y.; Antonietti, M. Synthesis of Very Small TiO₂ Nanocrystals in a Room-Temperature Ionic Liquid and Their Self-Assembly toward Mesoporous Spherical Aggregates. *J. Am. Chem. Soc.* **2003**, *125*, 14960–14961. [[CrossRef](#)] [[PubMed](#)]
84. Ma, Z.; Yu, J.; Dai, S. Preparation of inorganic materials using ionic liquids. *Adv. Mater.* **2010**, *22*, 261–285. [[CrossRef](#)] [[PubMed](#)]
85. Vioux, A.; Viau, L.; Volland, S.; Le Bideau, J. Use of ionic liquids in sol-gel; ionogels and applications. *Comptes Rendus Chim.* **2010**, *13*, 242–255. [[CrossRef](#)]
86. Viau, L.; Néouze, M.A.; Biolley, C.; Volland, S.; Brevet, D.; Gaveau, P.; Dieudonné, P.; Galarneau, A.; Vioux, A. Ionic liquid mediated sol-gel synthesis in the presence of water or formic acid: Which synthesis for which material? *Chem. Mater.* **2012**, *24*, 3128–3134. [[CrossRef](#)]
87. Verma, Y.L.; Singh, R.K.; Oh, I.-K.; Chandra, S. Ionic liquid template assisted synthesis of porous nano-silica nails. *R. Soc. Chem. Adv.* **2014**, *4*, 39978. [[CrossRef](#)]
88. Gupta, A.K.; Singh, R.K.; Chandra, S. Studies on mesoporous silica ionogels prepared by sol-gel method at different gelation temperatures. *R. Soc. Chem. Adv.* **2013**, *3*, 13869. [[CrossRef](#)]
89. Martinelli, A.; Nordstierna, L. An investigation of the sol-gel process in ionic liquid–silica gels by time resolved Raman and 1H NMR spectroscopy. *Phys. Chem. Chem. Phys.* **2012**, *14*, 13216. [[CrossRef](#)] [[PubMed](#)]
90. Martinelli, A. Effects of a protic ionic liquid on the reaction pathway during non-aqueous sol-gel synthesis of silica: A Raman spectroscopic investigation. *Int. J. Mol. Sci.* **2014**, *15*, 6488–6503. [[CrossRef](#)] [[PubMed](#)]
91. Ito, S.; Zakeeruddin, S.M.; Comte, P.; Liska, P.; Kuang, D.; Grätzel, M. Bifacial dye-sensitized solar cells based on an ionic liquid electrolyte. *Nat. Photonics* **2008**, *2*, 693–698. [[CrossRef](#)]
92. Singh, M.P.; Singh, R.K.; Chandra, S. Ionic liquids confined in porous matrices: Physicochemical properties and applications. *Prog. Mater. Sci.* **2014**, *64*, 73–120. [[CrossRef](#)]
93. Li, H.; Bhadury, P.S.; Song, B.; Yang, S. Immobilized functional ionic liquids: Efficient, green, and reusable catalysts. *R. Soc. Chem. Adv.* **2012**, *2*, 12525. [[CrossRef](#)]
94. Safaei, S.; Mohammadpour-baltork, I.; Khosropour, A.R.; Moghadam, M.; Tangestaninejad, S.; Mirkhani, V. Nano-silica supported acidic ionic liquid as an efficient catalyst for the multi-component synthesis of indazolophthalazine-triones and bis-indazolophthalazine-triones. *Catal. Sci. Technol.* **2013**, *3*, 2717–2722. [[CrossRef](#)]
95. Marins, J.A.; Soares, B.G.; Silva, A.A.; Livi, S. Silica prepared in the presence of alkylphosphonium-based ionic liquids and its performance in electrorheological fluids. *RSC Adv.* **2014**, *4*, 50925–50931. [[CrossRef](#)]
96. Marins, J.A.; Soares, B.G. Ionic liquid-based organically modified silica for the development of new electrorheological fluids. *Colloids Surf. A Physicochem. Eng. Asp.* **2017**, *529*, 311–319. [[CrossRef](#)]
97. Marins, J.A.; Soares, B.G.; Silva, A.A.; Hurtado, M.G.; Livi, S. Electrorheological and dielectric behavior of new ionic liquid/silica systems. *J. Colloid Interface Sci.* **2013**, *405*, 64–70. [[CrossRef](#)] [[PubMed](#)]
98. Matějka, L. Epoxy-silica/silsesquioxane Polymer Nanocomposites. In *Hybrid Nanocomposites for Nanotechnology*; Springer: Boston, MA, USA, 2009; pp. 1–84.

99. Mark, J.E.; Jiang, C.Y.; Tang, M.Y. Simultaneous curing and filling of elastomers. *Macromolecules* **1984**, *17*, 2613–2616. [[CrossRef](#)]
100. Landry, C.J.; Coltrain, B.K.; Brady, B.K. In situ polymerization of tetraethoxysilane in poly(methyl methacrylate): Morphology and dynamic mechanical properties. *Polymer* **1992**, *33*, 1486–1495. [[CrossRef](#)]
101. Bauer, B.J.; Liu, D.-W.; Jackson, C.L.; Barnes, J.D. Epoxy/SiO₂ Interpenetrating Polymer Networks. *Polym. Adv. Technol.* **1996**, *7*, 333–339. [[CrossRef](#)]
102. Matějka, L.; Dušek, K.; Pleštil, J.; Kříž, J.; Lednický, F. Formation and structure of the epoxy-silica hybrids. *Polymer* **1999**, *40*, 171–181. [[CrossRef](#)]
103. Matějka, L.; Dukh, O.; Meissner, B.; Hlavata, D.; Brus, J.; Strachota, A. Block Copolymer Organic-Inorganic Networks. Formation and Structure Ordering. *Macromolecules* **2003**, *36*, 7977–7985. [[CrossRef](#)]
104. Huang, H.H.; Orler, B.; Wilkes, G.L. Ceramers: Hybrid materials incorporating polymeric/oligomeric species with inorganic glasses by a sol-gel process. *Polym. Bull.* **1985**, *14*, 557–564. [[CrossRef](#)]
105. Kang, S.; Hong, S., II; Choe, C.R.; Park, M.; Rim, S.; Kim, J. Preparation and characterization of epoxy composites filled with functionalized nanosilica particles obtained via sol-gel process. *Polymer* **2001**, *42*, 879–887. [[CrossRef](#)]
106. Palza, H.; Vergara, R.; Zapata, P. Composites of polypropylene melt blended with synthesized silica nanoparticles. *Compos. Sci. Technol.* **2011**, *71*, 535–540. [[CrossRef](#)]
107. Rahman, I.A.; Padavettan, V. Synthesis of Silica nanoparticles by sol-gel: Size-dependent properties, surface modification, and applications in silica-polymer nanocomposites: A review. *J. Nanomater.* **2012**, *2012*, 132424. [[CrossRef](#)]
108. Tjong, S.C. Structural and mechanical properties of polymer nanocomposites. *Mater. Sci. Eng. R Rep.* **2006**, *53*, 73–197. [[CrossRef](#)]
109. Hussain, F.; Hojjati, M.; Okamoto, M.; Gorga, R.E. Review article: Polymer-matrix Nanocomposites, Processing, Manufacturing, and Application: An Overview. *J. Compos. Mater.* **2006**, *40*, 1511–1575. [[CrossRef](#)]
110. Kim, D.; Lee, J.S.; Barry, C.M.F.; Mead, J.L. Effect of fill factor and validation of characterizing the degree of mixing in polymer nanocomposites. *Polym. Eng. Sci.* **2007**, *47*, 2049–2056. [[CrossRef](#)]
111. Matějka, L.; Dukh, O.; Kolařík, J. Reinforcement of crosslinked rubbery epoxies by in-situ formed silica. *Polymer* **2000**, *41*, 1449–1459. [[CrossRef](#)]
112. Ponyrko, S.; Kobera, L.; Brus, J.; Matějka, L. Epoxy-silica hybrids by nonaqueous sol-gel process. *Polymer* **2013**, *54*, 6271–6282. [[CrossRef](#)]
113. Jain, S.; Goossens, H.; Picchioni, F.; Magusin, P.; Mezari, B.; Van Duin, M. Synthetic aspects and characterization of polypropylene-silica nanocomposites prepared via solid-state modification and sol-gel reactions. *Polymer* **2005**, *46*, 6666–6681. [[CrossRef](#)]
114. Wu, C.L.; Zhang, M.Q.; Rong, M.Z.; Friedrich, K. Silica nanoparticles filled polypropylene: Effects of particle surface treatment, matrix ductility and particle species on mechanical performance of the composites. *Compos. Sci. Technol.* **2005**, *65*, 635–645. [[CrossRef](#)]
115. Zhu, X.; Melian, C.; Dou, Q.; Peter, K.; Demco, D.E.; Möller, M.; Anokhin, D.V.; Le Meins, J.M.; Ivanov, D.A. Morphology of injection-molded isotactic polypropylene/silica composites prepared via in-situ sol-gel technology. *Macromolecules* **2010**, *43*, 6067–6074. [[CrossRef](#)]
116. Landry, C.; Coltrain, B.; Landry, M.; Fitzgerald, J.; Long, V. Poly (vinyl acetate)/Silica Filled Materials: Material Properties of in Situ vs Fumed Silica Particles. *Macromolecules* **1993**, *26*, 3702–3712. [[CrossRef](#)]
117. Kulkarni, S.S.; Kittur, A.A.; Aralaguppi, M.I.; Kariduraganavar, M.Y. Synthesis and characterization of hybrid membranes using poly(vinyl alcohol) and tetraethylorthosilicate for the pervaporation separation of water-isopropanol mixtures. *J. Appl. Polym. Sci.* **2004**, *94*, 1304–1315. [[CrossRef](#)]
118. Uragami, T.; Okazaki, K.; Matsugi, H.; Miyata, T. Structure and permeation characteristics of an aqueous ethanol solution of organic—Inorganic hybrid membranes composed of poly(vinyl alcohol) and tetraethoxysilane. *Macromolecules* **2002**, *35*, 9156–9163. [[CrossRef](#)]
119. Zhang, Q.G.; Liu, Q.L.; Huang, S.P.; Hu, W.W.; Zhu, A.M. Microstructure-related performances of poly(vinyl alcohol)-silica hybrid membranes: A molecular dynamics simulation study. *J. Mater. Chem.* **2012**, *22*, 10860. [[CrossRef](#)]
120. Silveira, K.F.; Yoshida, I.V.P.; Nunes, S.P. Phase separation in PMMA/silica sol-gel systems. *Polymer* **1995**, *36*, 1425–1434. [[CrossRef](#)]

121. Bokobza, L.; Diop, A.L. Reinforcement of Silicone Rubbers by Sol-Gel In Situ Generated Filler Particles. In *Rubber Nanocomposites: Preparation, Properties, and Applications*; John Wiley & Sons Ltd.: New York, NY, USA, 2010; pp. 63–85, ISBN 9780470823453.
122. Roy, N.; Bhowmick, A.K. Novel in situ Silica/Polydimethylsiloxane Nanocomposites: Facile One-Pot Synthesis and Characterization. *Rubber Chem. Technol.* **2012**, *85*, 92–107. [[CrossRef](#)]
123. Zhang, W.; Zhu, L.; Ye, H.; Liu, H.; Li, W. Modifying a waterborne polyacrylate coating with a silica sol for enhancing anti-fogging performance. *R. Soc. Chem. Adv.* **2016**, *6*, 92252–92258. [[CrossRef](#)]
124. Gao, J.G.; Lv, H.Q.; Zhang, X.F. Preparation and Properties of Emulsion Coating of Polyacrylate Modified by In-situ Nano-hybrid Silica. *Adv. Mater. Res.* **2011**, *239*, 3221–3224. [[CrossRef](#)]
125. Ajayan, P.M.; Schadler, L.S.; Braun, P.V. *Nanocomposite Science and Technology*; John Wiley & Sons: New York, NY, USA, 2003; Volume 230.
126. Ponyrko, S.; Kovářová, J.; Kobera, L.; Matějka, L. High-Tg, heat resistant epoxy-silica hybrids with a low content of silica generated by nonaqueous sol-gel process. *J. Appl. Polym. Sci.* **2014**, *131*. [[CrossRef](#)]
127. Carvalho, A.P.A.; Soares, B.G.; Livi, S. Organically modified silica (ORMOSIL) bearing imidazolium—Based ionic liquid prepared by hydrolysis/co-condensation of silane precursors: Synthesis, characterization and use in epoxy networks. *Eur. Polym. J.* **2016**, *83*, 311–322. [[CrossRef](#)]
128. Pereira, J.F.B.; Barber, P.S.; Kelley, S.P.; Berton, P.; Rogers, R.D. Double Salt Ionic Liquids Based on 1-Ethyl-3-Methylimidazolium Acetate and Hydroxyl-Functionalized Ammonium Acetates: Strong Effects of Weak Interactions. *Phys. Chem. Chem. Phys.* **2017**, *19*, 26934–26943. [[CrossRef](#)] [[PubMed](#)]
129. Lozano, L.J.; Godínez, C.; de los Ríos, A.P.; Hernández-Fernández, F.J.; Sánchez-Segado, S.; Alguacil, F.J. Recent advances in supported ionic liquid membrane technology. *J. Membr. Sci.* **2011**, *376*, 1–14. [[CrossRef](#)]
130. Dai, Z.; Noble, R.D.; Gin, D.L.; Zhang, X.; Deng, L. Combination of ionic liquids with membrane technology: A new approach for CO₂ separation. *J. Membr. Sci.* **2016**, *497*, 1–20. [[CrossRef](#)]
131. Hirota, Y.; Maeda, Y.; Yamamoto, Y.; Miyamoto, M.; Nishiyama, N. Organosilica membrane with ionic liquid properties for separation of toluene/H₂ mixture. *Materials* **2017**, *10*, 901. [[CrossRef](#)] [[PubMed](#)]
132. Tomé, L.C.; Mecerreyes, D.; Freire, C.S.R.; Rebelo, L.P.N.; Marrucho, I.M. Polymeric ionic liquid membranes containing IL–Ag⁺ for ethylene/ethane separation via olefin-facilitated transport. *J. Mater. Chem. A* **2014**, *2*, 5631. [[CrossRef](#)]
133. Luza, L.; Rambor, C.P.; Gual, A.; Bernardi, F.; Domingos, J.B.; Grehl, T.; Brüner, P.; Dupont, J. Catalytically Active Membranelike Devices: Ionic Liquid Hybrid Organosilicas Decorated with Palladium Nanoparticles. *Am. Chem. Soc. Catal.* **2016**, *6*, 6478–6486. [[CrossRef](#)]
134. Sun, J.-K.; Lin, H.-J.; Zhang, W.-Y.; Gao, M.-R.; Antonietti, M.; Yuan, J. A tale of two membranes: From poly(ionic liquid) to metal-organic framework hybrid nanoporous membranes via pseudomorphic replacement. *Mater. Horiz.* **2017**, *4*, 681–687. [[CrossRef](#)]
135. Tomé, L.C.; Marrucho, I.M. Ionic liquid-based materials: A platform to design engineered CO₂ separation membranes. *Chem. Soc. Rev.* **2016**, *45*, 2785–2824. [[CrossRef](#)] [[PubMed](#)]
136. Lendlein, A. (Ed.) *Advances in Polymer Science*. In *Shape-Memory Polymers*; Springer: Berlin/Heidelberg, Germany, 2010; Volume 226, ISBN 978-3-642-12358-0.
137. Behl, M.; Lendlein, A. Shape-memory polymers. *Mater. Today* **2007**, *10*, 20–28. [[CrossRef](#)]
138. Liu, C.; Qin, H.; Mather, P.T. Review of progress in shape-memory polymers. *J. Mater. Chem.* **2007**, *17*, 1543. [[CrossRef](#)]
139. Yuan, C.; Guo, J.; Yan, F. Shape memory poly(ionic liquid) gels controlled by host-guest interaction with β -cyclodextrin. *Polymer* **2014**, *55*, 3431–3435. [[CrossRef](#)]
140. Du, H.; Liu, X.; Yu, Y.; Xu, Y.; Wang, Y.; Liang, Z. Microwave-Induced Poly(ionic liquid)/Poly(vinyl alcohol) Shape Memory Composites. *Macromol. Chem. Phys.* **2016**, *217*, 2626–2634. [[CrossRef](#)]
141. Rossiter, J.; Takashima, K.; Mukai, T. Shape memory properties of ionic polymer-metal composites. *Smart Mater. Struct.* **2012**, *21*, 112002. [[CrossRef](#)]
142. Odent, J.; Raquez, J.M.; Samuel, C.; Barrau, S.; Enotiadis, A.; Dubois, P.; Giannelis, E.P. Shape-Memory Behavior of Polylactide/Silica Ionic Hybrids. *Macromolecules* **2017**, *50*, 2896–2905. [[CrossRef](#)]
143. White, S.R.; Sottos, N.R.; Geubelle, P.H.; Moore, J.S.; Kessler, M.R.; Sriram, S.R.; Brown, E.N.; Viswanathan, S. Autonomic healing of polymer composites. *Nature* **2001**, *409*, 794–797. [[CrossRef](#)] [[PubMed](#)]
144. Hayes, S.A.; Swait, T.J.; Lafferty, A.D. *Recent Advances in Smart Self-Healing Polymers and Composites*; Elsevier: Amsterdam, The Netherlands, 2015; ISBN 9781782422808.

145. Döhler, D.; Peterlik, H.; Binder, W.H. A dual crosslinked self-healing system: Supramolecular and covalent network formation of four-arm star polymers. *Polymer* **2014**, *69*, 264–273. [[CrossRef](#)]
146. Thakur, V.K.; Kessler, M.R. Self-healing polymer nanocomposite materials: A review. *Polymer* **2015**, *69*, 369–383. [[CrossRef](#)]
147. Luo, X.; Mather, P.T. Shape memory assisted self-healing coating. *Am. Chem. Soc. Macro Lett.* **2013**, *2*, 152–156. [[CrossRef](#)]
148. Nji, J.; Li, G. A biomimic shape memory polymer based self-healing particulate composite. *Polymer* **2010**, *51*, 6021–6029. [[CrossRef](#)]
149. Grigoriev, D.; Shchukina, E.; Shchukin, D.G. Nanocontainers for Self-Healing Coatings. *Adv. Mater. Interfaces* **2017**, *4*, 1600318. [[CrossRef](#)]
150. Kalista, S.J.; Pflug, J.R.; Varley, R.J. Effect of ionic content on ballistic self-healing in EMAA copolymers and ionomers. *Polym. Chem.* **2013**, *4*, 4910. [[CrossRef](#)]
151. Ueki, T.; Usui, R.; Kitazawa, Y.; Lodge, T.P.; Watanabe, M. Thermally Reversible Ion Gels with Photohealing Properties Based on Triblock Copolymer Self-Assembly. *Macromolecules* **2015**, *48*, 5928–5933. [[CrossRef](#)]
152. Saurín, N.; Sanes, J.; Carrión, F.J.; Bermúdez, M.D. Self-healing of abrasion damage on epoxy resin controlled by ionic liquid. *R. Soc. Chem. Adv.* **2016**, *6*, 37258–37264. [[CrossRef](#)]
153. Cao, Y.; Morrissey, T.G.; Acome, E.; Allec, S.I.; Wong, B.M.; Keplinger, C.; Wang, C. A Transparent, Self-Healing, Highly Stretchable Ionic Conductor. *Adv. Mater.* **2017**, *29*, 1605099. [[CrossRef](#)] [[PubMed](#)]
154. Cuthbert, T.J.; Jadischke, J.J.; De Bruyn, J.R.; Ragogna, P.J.; Gillies, E.R. Self-Healing Polyphosphonium Ionic Networks. *Macromolecules* **2017**, *50*, 5253–5260. [[CrossRef](#)]
155. Das, A.; Sallat, A.; Böhme, F.; Suckow, M.; Basu, D.; Wießner, S.; Stöckelhuber, K.W.; Voit, B.; Heinrich, G. Ionic Modification Turns Commercial Rubber into a Self-Healing Material. *Am. Chem. Soc. Appl. Mater. Interfaces* **2015**, *7*, 20623–20630. [[CrossRef](#)] [[PubMed](#)]
156. Odent, J.; Raquez, J.-M.; Dubois, P.; Giannelis, E.P. Ultra-stretchable ionic nanocomposites: From dynamic bonding to multi-responsive behavior. *J. Mater. Chem. A* **2017**, *5*, 13357–13363. [[CrossRef](#)]



© 2017 by the authors. Licensee MDPI, Basel, Switzerland. This article is an open access article distributed under the terms and conditions of the Creative Commons Attribution (CC BY) license (<http://creativecommons.org/licenses/by/4.0/>).